Cofilin1 driven actin dynamics controls migration of thymocytes and is essential for positive selection in the thymus

Andree Salz, Christine Gurniak, Friederike Jönsson, Walter Witke

Cofilin1 driven actin dynamics controls migration of thymocytes and is essential for positive selection in the thymus

Andree Salz[1], Christine Gurniak[1], Friederike Jönsson[2] and Walter Witke[1*]

[1]Institute of Genetics, University of Bonn

[2] Unit of Antibodies in Therapy and Pathology, Institut Pasteur, UMR 1222 INSERM, 75015 Paris, France

*Correspondence: w.witke@uni-bonn.de (W.W.)

Prof. Dr. Walter Witke

Institute of Genetics, University Bonn

Karlrobert-Kreiten Strasse 13

53115 Bonn

e-mail: w.witke@uni-bonn.de

phone: +49 228 734210

FAX: +49 228 734263

Key words: cofilin1, actin filament turnover, cell migration, T cell development

Summary statement: Our results show that cofilin1 controlled migration patterns are essential for positive selection of thymocytes and differentiation into T cells

JCS Advance Online Article. Posted on 23 January 2020

Abstract

Actin dynamics is essential for T cell development. We show here that cofilin1 is the key molecule for controlling actin filament turnover in this process. Mice with specific depletion of cofilin1 in thymocytes showed increased steady state levels of actin filaments, and associated alterations in the pattern of thymocyte migration and adhesion. Our data suggest that cofilin1 is controlling oscillatory F-actin changes, a parameter that influences the migration pattern in a 3-D environment. In a collagen matrix, cofilin1 controls the speed and resting intervals of migrating thymocytes. Cofilin1 was not involved in thymocyte proliferation, cell survival, apoptosis, or surface receptor trafficking. However, in cofilin1 mutant mice impaired adhesion and migration resulted in a specific block of thymocyte differentiation from CD4/CD8 double positive thymocytes towards CD4 and CD8 single positive cells. Our data suggest that tuning of the dwelling time of thymocytes in the thymic niches is tightly controlled by cofilin1 and essential for positive selection during T cell differentiation. We describe a novel role of cofilin1 in the physiological context of migration dependent cell differentiation.

Introduction

Differentiation of α,β T cells follows a complex sequence of molecular events that take place in spatially defined niches of the thymus. T cell development comprises several distinct stages, each of which is tightly regulated to generate mature and non-self-reactive T lymphocytes: $CD4^-/CD8^-$ double negative (DN) precursors develop into $CD4^+/CD8^+$ double positive (DP) cells, before they finally differentiate into $CD4^+$ (CD4SP) or $CD8^+$ (CD8SP) single positive thymocytes. The DN cell population can be further characterized by the expression of CD25 and CD44 (Ceredig and Rolink, 2002; Godfrey et al., 1993), or functionally by a rearranged T cell receptor (TCR) β locus. After successful β-chain arrangement and expression of a functional pre-T cell receptor, DN thymocytes rapidly proliferate into double-positive DP cells and express markers such as CD69 (Von Boehmer et al., 1999). DP cells next undergo TCRα chain gene re-arrangement, in order to assemble the final α,β TCR complex, which is required for positive and negative selection and generation of CD4 or CD8 single positive (SP) thymocytes (Jameson and Bevan, 1998; Sebzda et al., 1999). Only then SP thymocytes are licensed to exit the thymus and to constitute the T cell compartments of the immune system.

Work from many groups has shown that T cell development is not simply following an autonomous programme, but rather depends on defined spatial cues provided by cell-cell contacts with epithelial stroma cells in the thymus. In this process thymocytes were found to follow a distinct migratory path between certain areas in the thymus (Lind et al., 2001; Porritt et al., 2003). In the cortex, $CD4^+/CD8^+$ thymocytes recognise MHC ligands on thymic epithelial cells. After successful positive selection, thymocytes then migrate to the central medullary region where they undergo negative selection (Anderson and Jenkinson, 2001) and elimination of thymocytes which recognise self-peptide-MHC on dendritic and medullary epithelial cells (Le Borgne et al., 2009). To coordinate this process the cortical and medullary compartments produce distinct chemokines including SDF-1α and CCL25 (Ladi et al., 2006; Love and Bhandoola, 2011; Takahama, 2006), and provide integrin mediated adhesion through LFA1/ICAM-1 (Fine and Kruisbeek, 1991).

Mutations affecting chemokine signaling or disturbing adhesion can lead to severe changes in thymocyte development (Lancaster et al., 2018; Savino et al., 2004; Uehara

et al., 2002a; Uehara et al., 2002b). Interestingly, many of these pathways are located upstream of cytoskeletal dynamics. For example, small GTPases are components of the main signaling pathways to cytoskeletal dynamics and have been shown to regulate thymocyte development (Cleverley et al., 1999; Galandrini et al., 1997), Rac-1 specifically positive and negative selection (Gomez et al., 2001), and WASP was shown to control thymocyte development (Zhang et al., 2002).

Furthermore, T cell activation through the TCR requires a scaffold of actin filaments (Bunnell et al., 2001; Dustin and Cooper, 2000; Monks et al., 1998; Samstag et al., 2003). Actin polymerisation was shown to be required for T cell polarization (Delon et al., 1998; Stradal et al., 2006), the formation of the contact zone (Sechi and Wehland, 2004), and T cell activation via calcium flux, IL-2 production and proliferation (Penninger and Crabtree, 1999). Cell adhesion through integrins was shown to be stabilized by the actin cytoskeleton (Brakebusch and Fässler, 2003). Actin nucleation-promoting factors such as the Abi/WAVE complex or Ena/Vasp can control TCR-mediated actin dynamics (Krause et al., 2000; Nolz et al., 2006; Zipfel et al., 2006). In conclusion, mutations in regulators of the cytoskeleton were shown to cause profound defects in lymphocyte function (Billadeau et al., 2007).

However, little is known about the actual mechanisms, by which actin binding proteins translate the signals into T cell function. To tackle this question, we need to focus on the downstream effector proteins that directly induce actin filament growth and shrinking. In this context the F-actin depolymerising proteins of the ADF/cofilin family are among the best studied molecules. ADF/cofilin members control the on- and off-rate of actin monomers from the filament ends (Carlier et al., 1997), and preferentially sever old (ADP-rich) actin filaments (Maciver et al., 1991; McGough et al., 1997). In mouse and human three genes, cofilin1, cofilin2 and ADF are encoded in the genome. They differ in their activities, expression pattern and biological functions (Nakashima et al., 2005; Vartiainen, 2002). ADF/cofilin were shown to control motility in cultured fibroblast and carcinoma cells (Ghosh et al., 2004; Kato et al., 2008), as well as in human CD4 T cells and Jurkat cells (Nishita et al., 2005; Xu et al., 2012).

Systemic deletion of cofilin1 in the mouse was shown to be embryonic lethal (Gurniak et al., 2005), a cofilin2 mutation resulted in a severe myopathy phenotype (Gurniak et al., 2014), while ADF deficient mice were viable (Bellenchi et al., 2007). These genetic studies indicated that cofilin1 cannot be functionally replaced by the other two

ADF/cofilin members. Indeed, in macrophages chemotaxis, adhesion, and antigen presentation were shown to depend on cofilin1 (Jönsson et al., 2012; Matsui et al., 2001), and in mature T cells cofilin1 was shown to provide a link between co-stimulation and the concomitant rearrangement of the actin cytoskeleton (Lee et al., 2000; Samstag et al., 2003). Cofilin1 has been studied with respect to T cell activation, however its function in the classical differentiation of α/β T cells in the thymus has been addressed only recently. It was shown that expression of a mutated cofilin1 protein can block T cell differentiation already at the DN stage (Seeland et al., 2018).

Here we show a new function of cofilin1 as a pacemaker of thymocyte migration and T cell differentiation in the thymus. Our data identify the turnover of actin filaments as a central mechanism in T cell development. We also present a mechanism by which cofilin1 controlled resting cycles can affect cell-cell interactions essential for the differentiation of DP thymocytes into mature SP T cells.

Results

Cofilin1 controls actin polymerisation cycles and steady state levels of F-actin in thymocytes

The aim of our experimental strategy was to genetically interfere with actin dynamics in developing thymocytes by slowing down actin filament turnover. We have shown previously that among the three cofilin/ADF genes, cofilin1 is the predominant actin filament severing factor in hematopoietic cell types (Jönsson et al., 2012). Using isoform specific antibodies for ADF, cofilin1 and cofilin2, we confirm here that only cofilin1 was expressed in thymocytes, while ADF and cofilin2 could not be detected (Fig. 1A). In thymocytes, cofilin1 expression was found to be developmentally regulated (Fig. 1B). While expressed at very low levels in CD4/CD8 double negative thymocytes (DN), cofilin1 expression increases in CD4/CD8 double positive thymocytes (DP), and reaches its highest expression in CD4 or CD8 single positive thymocytes (CD4SP, CD8SP). Interestingly, also total actin levels were found to fluctuate significantly during thymocyte differentiation, resulting in the highest cofilin1/actin ratio in DP thymocytes. Deletion of cofilin1 in thymocytes should therefore be an ideal tool to blunt actin dynamics in T cell development *in vivo*.

To achieve this, we crossed mice carrying a floxed cofilin1 allele (Gurniak et al., 2005) (Fig. 1C) to a CD4-cre transgenic mouse line expressing cre-recombinase in early thymocytes starting at the DN3 stage (Wolfer et al., 2001). Using a Rosa26-Stop-YFP reporter line (Srinivas et al., 2001), we confirmed CD4-cre mediated deletion already at the DN stage (22% deletion), which then increased to 83% in DP cells, and finally reached 99% in CD4SP thymocytes (Fig. 1D). In agreement with the YFP-reporter gene activation, the floxed cofilin1 allele was deleted with high efficiency in thymocytes of $Cof1^{fl//fl,CD4cre}$ mice (Fig. 1E). In total thymocytes, recombination of the floxed cofilin1 allele (fl) had occurred with an efficiency of more than 95% (Δ) as judged by Southern Blot analysis. This analysis also confirmed the specificity of cofilin1 deletion in thymocytes, but not in other tissues (Fig. 1E). Concomitantly, cofilin1 protein was depleted in $Cof1^{fl//fl,CD4cre}$ total thymocytes by more than 90% as shown by Western blot analyses (Fig. 1F).

Importantly, the deletion of cofilin1 did not result in any compensatory upregulation of ADF, cofilin2, or other related F-actin binding proteins, such as for example gelsolin or CapG (Fig. 1F). With the depletion of cofilin1, we consequently removed all ADF/cofilin activity from DP thymocytes. Actin filament dynamics should therefore be severely tuned down. To formally test this assumption, we isolated primary thymocytes from $Cof1^{fl/fl,CD4cre}$ mice and measured their F-actin and G-actin levels, using fluorescently labeled phalloidin as a sensor for F-actin and fluorescently labeled DNaseI to detect G-actin. Quantitation by FACS analysis revealed a 2.5-fold increase in F-actin levels when compared to control thymocytes (Fig. 2A). The increase in F-actin was paralleled by a reduction of the G-actin pool. Quantitation of F/G-actin levels by fluorescence is very sensitive, but will only allow to measure relative changes. To obtain an estimate of the absolute F-actin and G-actin levels, we biochemically separated the Triton-X100 insoluble (F-actin) and soluble (G-actin) actin pool and determined their amounts by Western blot (Watts and Howard, 1993). In agreement with the FACS data, also the biochemical fractionation showed an increase in F-actin and decrease of G-actin in cofilin1 depleted thymocytes (Fig. 2B). Considering the absolute actin levels, the mutant thymocytes still contained about 60% G-actin. In comparison control thymocytes contained about 80% G-actin (Fig. 2B). Although cofilin1 depleted thymocytes still had significant G-actin levels, one important question was whether this monomeric actin pool would still be polymerisation competent upon cell activation.

Therefore, we monitored the actual kinetics of actin polymerisation and depolymerisation after stimulation of thymocytes with the chemokine SDF-1α (Fig. 2C). With this assay we were able to resolve actin polymerisation within seconds and to monitor cycles of F-actin formation over longer periods. Cycling of F-actin levels in stimulated cells is a general phenomenon that in fact had been described some time ago (McRobbie and Newell, 1983). In our hands, control thymocytes showed an oscillatory pattern of F-actin levels, with an initial peak around 5 seconds after stimulation, followed by a second slower rise within the next 30 seconds and a subsequent return to baseline levels within 1-2 minutes. For cofilin1 depleted thymocytes a number of interesting differences were observed: First, thymocytes lacking cofilin1 could polymerise actin upon stimulation, and the F-actin peak increased within 10 seconds. Second, the initial F-actin increase was significantly exaggerated in cofilin1 depleted thymocytes when compared to control thymocytes. And third, the increased F-actin levels of $Cof1^{fl/fl,CD4cre}$ thymocytes never returned to baseline, even beyond the 5 minutes end point of the experiment (Fig. 2C). These findings suggest that cofilin1 function is essential to limit the activity of the actin polymerisation machinery. Without cofilin1 activity actin filament dynamics becomes more refractory to stimulation.

Taken together, we developed and validated a genetic model system that allows to block actin filament dynamics specifically at the DP stage of thymocyte development *in vivo*. We next focused on our main question how actin dynamics is linked to thymocyte development.

Cofilin1 is essential for positive selection in the thymus and the transition of DP cells to $CD4^+$ and $CD8^+$ SP cells

In the thymus, precursor cells pass several checkpoints on the way to functional T cells. The critical steps are characterised by the sequential expression of the T cell receptor (TCR) associated co-receptors CD4 and CD8. First, immature double negative (DN) thymocytes proceed to the double positive (DP) stage, which represents close to 90% of thymocytes. In the final differentiation step, DP cells differentiate towards single positive cells (SP), which express either CD4 or CD8. Mature T cells can then exit the thymus and home to peripheral secondary lymphatic organs.

In Cof1$^{fl/fl,CD4cre}$ mice the total number of thymocytes was unchanged (Fig. 3A), suggesting that the deletion of cofilin1 did not have any major adverse effect on proliferation or survival of thymocytes. However, we observed a severe differentiation block from DP cells to SP cells. FACS analysis showed that the thymus of Cof1$^{fl/fl,CD4cre}$ mice was practically devoid of CD4SP and CD8SP thymocytes (Fig. 3B). Since DN and DP cells were not affected in Cof1$^{fl/fl,CD4cre}$ mice, the differentiation block must occur at the transition from DP to SP cells (Fig. 3C). Lineage commitment to CD4SP and CD8SP cells occurs at the late stage of positive selection of DP thymocytes that only survive if they receive a productive signal through their re-arranged TCR (Swat et al., 1993; Yamashita et al., 1993). Cells that have been successfully selected, express high levels of the T cell receptor β-chain (TCRß^{high}) and the activation marker CD69 (CD69^{+}). In Cof1$^{fl/fl,CD4cre}$ thymocytes we found a dramatic reduction of the TCRß^{high}/CD69^{+} subpopulation (Fig. 3D), suggesting that cofilin1 is critical for the processes involved in positive selection.

The lack of SP thymocytes was further illustrated by the anatomy of the thymus from Cof1$^{fl/fl,CD4cre}$ mice (Fig. 3E). The area of the cortex was expanded at the expense of the medullary compartment, while the overall size of the thymus was unchanged. The medullary structures were nearly absent in cofilin1 mutant mice, only small fragmented residual islands could be identified (Fig. 3E). The reduction of the medullary compartment is in agreement with the loss of CD4SP and CD8SP thymocytes, since SP thymocytes were shown to support the maintenance of the medulla as a niche (Negishi et al., 1995; Philpott et al., 1992).

Only mature SP T cells will exit the thymus and home into secondary lymphatic organs. However, despite the block in thymocyte development we found a small number of SP T cells in lymph nodes, spleen and blood of Cof1$^{fl/fl,CD4cre}$ mice (Fig. 4 A,B). This raised the question on the nature of these T cells that reached about 10% of normal T cell counts. Were these cofilin1 deleted T cells that had possibly left the thymus?

Expression analyses clarified that the peripheral T cells in Cof1$^{fl/fl,CD4cre}$ mice in fact were not deleted for the cofilin1 gene and expressed cofilin1 protein. This was illustrated by Western blot (Fig. 4C), as well as Southern blot analyses of CD4-sorted peripheral T cells from Cof1$^{fl/\Delta,CD4cre}$ mice (Fig. 4D). The rational to use Cof1$^{fl/\Delta,CD4cre}$ mice for this experiment was to better illustrate the lack of deletion by the equal signal intensities of fl- and Δ alleles. If complete deletion would have occurred the fl-signal

should have disappeared, if partial deletion would have occurred the fl-signal should diminish and the Δ allele increase. The equal ratio of the fl and Δ alleles indicated that basically none of the fl-alleles was converted to the Δ allele and that practically all the T cells found in the periphery had escaped cofilin1 gene deletion (Fig. 4D).

The presence of functional escaper T cells in the periphery also showed that the differentiation block is a cell autonomous phenomenon of mutant thymocytes and not caused by alterations in the thymic stroma environment. These data show that T cells can still emerge from a morphologically altered thymus as long as they express cofilin1. The low abundance of T cells in secondary lymphatic organs of Cof1$^{fl/fl,CD4cre}$ mice (Fig. 4B) did not affect the B cell representation as shown by CD19-positive cells in lymph node as an example (Fig. 4E). One should note that the apparent increase of B cells in the FACS plot is owed to the representation of relative numbers of T cells and B cells. The absolute numbers of B cells in lymph nodes of mutant and control mice are in fact not significantly altered (Suppl. Fig. E).

Thymocyte proliferation and apoptosis are independent of cofilin1

We next addressed the underlying mechanisms responsible for the differentiation block and the severe reduction of T cells in Cof1$^{fl/fl,CD4cre}$ mutants. One trivial explanation could simply be a block in thymocyte proliferation and/or increased cell death.

The total cell counts in the thymus of Cof1$^{fl/fl,CD4cre}$ mutants and control mice were identical, as well as the pools of DN and DP thymocytes (see Fig. 3 A,C). This suggested, that alterations of the proliferation and apoptosis equilibrium were unlikely to account for the block in thymocyte development. Nonetheless, we quantitated apoptosis in isolated total thymocytes as well as DP cells, using active caspase 3 specific antibodies. We did not observe any significant difference between control mice and Cof1$^{fl/fl,CD4cre}$ mutant mice (Fig. 5 A,B). In steady state conditions, apoptotic cells in the thymus are cleared very rapidly and therefore it might be difficult to detect small changes in apoptotic numbers. To uncover a possibly mild phenotype we challenged isolated total thymocytes by *in vitro* culture before measuring apoptosis. Even under these conditions, we did not find any increase of apoptosis in cofilin1 depleted thymocytes using Annexin V as a marker (Fig. 5B).

To address the proliferation potential, we cultured total thymocytes in the presence of PMA/Ionomycin as growth stimulators. Both, control thymocytes as well as cofilin1

depleted thymocytes showed comparable cell expansion *in vitro* (Fig. 5C). In addition, cell cycle analysis ruled out any defect in cytokinesis as indicated by the normal cell distribution in G0/G1- and G2/M-phases (Fig. 5D).

Collectively, these data show that cofilin1 deficiency does not promote apoptosis in thymocytes, nor does it affect cell proliferation.

In thymocytes cofilin1 is not required for surface receptor turnover

One critical parameter in T cell development is the sequential up- and downregulation of surface receptors such as CD4 and CD8, or the T cell receptor chains (Guidos et al., 1990; Malissen and Malissen, 1996). Previously, cofilin1 was shown to control receptor trafficking in neuronal cells (Rust et al., 2010), and we therefore hypothesized that cofilin1 might similarly be involved in surface receptor turnover in thymocytes. Any impairment could contribute to the differentiation block in $Cof1^{fl/fl,CD4cre}$ mutant mice.

We examined whether cofilin1 contributed to the turnover of CD4 and CD8 on the cell surface. First, all surface receptors were stripped from the outer surface of thymocytes by protease treatment, followed by a recovery period at 37°C, during which we monitored the re-appearance of CD4 and CD8 molecules on the cell surface. In this assay $Cof1^{fl/fl,CD4cre}$ thymocytes and control cells, both recovered CD4 and CD8 (Fig. 5E). Furthermore, the kinetics of CD4 and CD8 receptors trafficking back to the surface were comparable as shown in a time course experiment over 14 hours (Fig. 5F). At 4°C receptor recovery was blocked in control and cofilin1 depleted thymocytes, proving that the underlying process was a physiological and active transport mechanism.

In summary, our data show that thymocytes do not require cofilin1 for CD4/CD8 receptor trafficking. It is therefore unlikely that CD4/CD8 receptor turnover contributes to the block in thymocyte development.

Cofilin1 is controlling cell adhesion and 3-D migration of thymocytes

Double positive thymocytes mature along a migratory path through the thymus. On the way through the cortex and the medulla, thymocytes receive signals via cell-cell contacts that are essential for their differentiation. Consequently, cell adhesion is a critical parameter in thymocyte development. For example, the interaction of thymocyte LFA-1 with epithelial cell ICAM-1 is one important pathway for T cell differentiation (Fine and Kruisbeek, 1991; Lub et al., 1997). Chemokines such as SDF-1α and CCL25,

both produced by stromal cells, play a pivotal role in integrin mediated thymocyte adhesion and development (Norment and Bevan, 2000; Peled et al., 2000; Uehara et al., 2002a).

We therefore tested whether cofilin1 deficiency affects thymocyte adhesion to ICAM-1. Without stimulation, as well as in presence of SDF-1α adhesion to ICAM-1 was strongly impaired in cofilin1 depleted thymocytes (Fig. 6A). In addition, SDF-1α stimulation could augment the percentage of adhering control thymocytes, while cofilin1 deficient thymocytes did not respond to the chemokine. Similar results were obtained when we measured thymocyte spreading on ICAM-1 coated surfaces. Spreading goes hand in hand with adhesion and strictly depends on the re-organisation of the actin cytoskeleton (Brakebusch and Fässler, 2003; Stossel, 1993). As seen for adhesion, also spreading was impaired in cofilin1 deficient thymocytes and cells did not respond to SDF-1α (Fig. 6B). It is noteworthy that the levels of ICAM-1 receptors were not changed in cofilin1 deficient thymocytes as shown by FACS analysis of LFA-1 subunit chains CD11a and CD18 (Suppl. Fig. A).

Adhesion and spreading are critical for cell migration. Most cells go through cycles of attaching, spreading and leading-edge protrusion, followed by cell rounding and pausing before another migration cycle is re-initiated (Friedl et al., 2001). Having identified cofilin1 as a parameter for thymocyte spreading and adhesion, we wanted to directly address cofilin1 function in thymocyte migration. To this aim we employed two conceptually different migration assays, which allowed us to dissect cell motility on hard surfaces as well as in softer three-dimensional substrates. A transwell-assay was performed to address chemotaxis in surface dependent motility, whereas a collagen matrix was used to investigate migration in 3-D. In both assays we used SDF-1α and CCL25, the two most abundant chemokines in the thymic cortex, to stimulate migration (Wurbel et al., 2000; Zaitseva et al., 1998).

Unstimulated migration of cofilin1 deficient thymocytes was significantly reduced in the transwell-assay (Fig. 6C). Likewise, chemotaxis towards the applied chemokines was impaired, despite the fact that cofilin1 depleted thymocytes showed increased migration as compared to medium control (Fig. 6C). We again validated that the respective chemokine receptors for SDF-1α (CD184/CXCR4) and CCL25 (CD199/CCR9) were indeed expressed at comparable levels on the surface of $Cof1^{fl/fl,CD4cre}$ and control thymocytes (Suppl. Fig. B). These results suggest, that the

impairment in cell motility is most likely downstream of signaling pathways, directly at the level of cofilin1 mediated actin filament dynamics. This is in good agreement with our initial observation on SDF-1α induced F-actin polymerisation (see Fig. 2C).

The importance of cofilin1 for cell migration was even more evident when we assayed migration in a three-dimensional environment. Here, random migration of cofilin1 depleted thymocytes was strongly impaired and also chemokine stimulated migration was severely compromised when compared to control cells (Fig. 6D). Live tracking of individual cells revealed that the average velocity of cofilin1 deficient thymocytes was significantly lower when compared to control cells (Fig. 6E). This is visually illustrated in a track plot were the path of individual Cof1$^{fl/fl,CD4cre}$ cells is marked in red in comparison to control thymocytes in black (Fig. 6F). To refine our analysis we determined the speed distribution of thymocytes over a period of 6 hours by binning of cells that moved at a certain speed. This analysis enables to appreciate what proportion of cells is migrating at a given speed (Fig. 6G). Our results illustrated that cofilin1 deficient thymocytes prefer to crawl at low speed and spend comparably little time migrating at higher velocity. Cof1$^{fl/fl,CD4cre}$ thymocytes preferentially moved in the low velocity range of 0.5-1.5 μm/min, while control thymocytes rather migrated in the high-speed range. Interestingly, the maximum velocity mutant thymocytes could reach was similar to control cells (Fig. 6H, left panel). Second, the persistence of directed migration was comparable for Cof1$^{fl/fl,CD4cre}$ and control cells, meaning that cofilin1 deficient thymocytes did not meander more than control cells (Fig. 6H, middle panel). Conversely, cofilin1 depleted thymocytes showed significantly prolonged resting intervals between the migration cycles (Fig. 6H, right panel). Generally speaking, mutant thymocytes were pausing longer on their migratory path, and once they were moving they migrated slower than control thymocytes. It is important to note that also control thymocytes use a ‘stop-and-go’ fashion, indicating the importance of this mode of migration in a physiological context and possibly thymocyte development.

In conclusion, our results provide new insights into the role of cofilin1 in 3-D cell migration. Cofilin1 is controlling adhesion, the pattern of migration cycles, and the average velocity of thymocytes. Together, these very specific alterations mount in the failure of thymocyte development *in vivo*.

Thymocyte differentiation can be uncoupled from cofilin1 dependent migration *in vitro*

Our results strongly argue for a cofilin1 dependent 'motility pattern' as the determining parameter for thymocyte differentiation *in vivo*. One prediction would then be that all cell inherent differentiation parameters, such as signaling mechanisms or gene expression patterns should function independently of cofilin1. If this was true, we should be able to circumvent the migration dependent differentiation block by providing the relevant external signals *in vitro*. This should then allow cofilin1 depleted DP thymocytes to differentiate towards SP thymocytes.

To address this final hypothesis and to test the uncoupling of differentiation from migration, we set up an *ex vivo* differentiation experiment. It was shown that incubation of DP thymocytes with a mix of TCRß/CD2 antibodies can mimic positive selection and push thymocyte differentiation predominantly towards $CD4^+$ single positive cells (Cibotti et al., 1997). Following this strategy, we stimulated thymocytes for 32 hours in culture and tested the conversion of DP towards SP cells. In our hands, more than 50% of control DP thymocytes differentiated into CD4SP cells (Fig. 7A). Similarly, more than 50% of $Cof1^{fl/fl,CD4cre}$ thymocytes converted to CD4SP cells (Fig. 7B). The same result was obtained when *in vitro* differentiation was triggered by increase of intracellular calcium via PMA/Ionomycin treatment (data not shown) (Mitnacht et al., 1998; Ohoka et al., 1996). These data demonstrated that cofilin1 deficient DP thymocytes have the full capacity to differentiate into SP cells.

In summary, our data demonstrate that cofilin1 is central to regulate a 'stop-and-go' mode of thymocyte migration and adhesion, which in a physiological context appears to be essential for providing environmental cues and cell interactions necessary for thymocyte differentiation.

Discussion

Imaging experiments performed in the thymus suggested that thymocyte migration is an important parameter for differentiation. For example, thymocytes depend on environmental cues provided by cell-cell contacts with epithelial stroma cells (Takahama, 2006), and during positive selection thymocytes migrate with defined

pausing cycles that allow interaction with MHC-expressing epithelial cells (Sebzda et al., 1999).

However, it has remained unclear, how these specific aspects of thymocyte motility are tuned on the level of the actin cytoskeleton. Signaling pathways controlling cytoskeletal dynamics have been identified, and mutations of WASP (Zhang et al., 2002), Rac-1 (Gomez et al., 2001), and other small GTPase pathways have suggested a link to actin (Costello et al., 2000). It is however difficult to unequivocally link these data to actin dynamics, as all of the mentioned targets entertain a crosstalk with numerous other cellular processes that might very well influence thymocyte differentiation, independent of actin regulation.

We therefore developed strategies to study the direct link of actin filament dynamics to thymocyte migration and differentiation. It was our objective to down-regulate actin filament turnover specifically in thymocytes, without interfering with any upstream signaling pathways or any other second cell type. Key to this strategy was to blunt all actin filament depolymerising activity by deleting cofilin1.

Cofilin1 is a member of a family of actin depolymerising factors, and the only ADF/cofilin protein expressed in thymocytes. Previous work from our group has identified cofilin1 as the central actin filament severing activity *in vivo* (Flynn et al., 2012; Jönsson et al., 2012). Related actin filament severing proteins such as gelsolin are not relevant for the here presented study, since gelsolin is expressed at very low levels, and previous work had excluded any important role in T cell development (Witke et al., 1995).

Cell type specific deletion of cofilin1 therefore provided an excellent tool to address actin filament dynamics in thymocyte development. We generated a conditional $Cof1^{fl/fl,CD4cre}$ mouse model, in which cofilin1 gene deletion occurred with high efficiency in early DP T cell precursors in the thymus. It is an intrinsic property to the hematopoietic system that even high cre-recombinase expression rates of more than 99% will allow a small number of cells to escape recombination and hence to maintain expression of the target gene. In this study, we indeed observed a small percentage of 'escaper cells', which expressed cofilin1 and developed normally into mature CD4 and CD8 T cells. This escaper fraction in fact served as a convenient control for supporting the cell autonomous function of cofilin1 in thymocytes (see below).

Upon deletion of cofilin1, neither ADF nor cofilin2 expression was found to compensate its absence in thymocytes. In agreement with the overall loss of severing activity, we

observed a pronounced increase in the F-actin content in thymocytes. Interestingly, the mutant thymocytes were still able to trigger actin polymerisation upon stimulation, suggesting that the mechanisms of actin nucleation and polymerisation can work independently of cofilin1, as long as a sufficient pool of polymerisation competent G-actin is available. In this context it is important to note that G-actin pools can be very different, depending on the cell type. For example, classical adherent cells such as fibroblasts have roughly 50% F-actin and 50% G-actin (Phillips et al., 1980). In resting thymocytes on the other hand, we found that only 20% of total actin is in the filamentous form, leaving 80% as monomeric G-actin pool. Despite the F-actin increase in cofilin1 deficient thymocytes, this still leaves about 60% of cellular actin to the G-actin pool. More important than steady-state levels of F/G-actin were the dynamic changes of F-actin, namely the actin polymerisation and depolymerisation kinetics. When cofilin1 was deleted, stimulation of actin polymerisation in thymocytes resulted in overshooting F-actin levels, which did not return to baseline levels during the timeframe of the experiment. Therefore, one major function of cofilin1 appears to be to counteract the polymerisation burst in a feedback loop, which ultimately allows an oscillating mode of actin polymerisation and depolymerisation. It is important to note that in our experiments we followed global actin polymerisation in the cell.

What are oscillatory F-actin fluctuations good for, and what is their possible role in a physiological context? Thymocytes have to migrate through the thymic epithelial tissue in order to sense local chemokines and interact with stromal signals to differentiate into mature T lymphocytes (Savino et al., 2004). Two photon studies on thymic tissue have shown that thymocytes exhibit mainly random walking through the cortex until they undergo selection, which appears to trigger a rapid directed migration towards the medulla (Witt et al., 2005). This implies that a sophisticated modulation of migration patterns is a major parameter of thymocyte differentiation.

With this in mind we can picture cofilin1 function in the thymus. Without cofilin1 DP thymocytes are developmentally arrested and do not differentiate into CD4SP and CD8SP thymocytes. Our data show that this phenomenon is associated with the lack of F-actin oscillations, that in return cause an unusual ‘motility pattern’ of cofilin1 deficient thymocytes. In a 3-D matrix this is illustrated by the prolonged pausing and lower migratory speed of $Cof1^{fl/fl,CD4cre}$ thymocytes. In addition, integrin mediated cell adhesion and spreading of thymocytes is dependent on cofilin1. The combined

migration and adhesion defects we observed *ex vivo*, however become critical *in vivo* in the tissue context. Apparently, cofilin1 is required for stirring thymocytes through the thymus and to allow cell-cell contacts to occur in a coordinated fashion. All our data presented here are in good agreement with this hypothesis. Cofilin1 depleted thymocytes miss these cues, but can be forced to differentiate into SP thymocytes simply by activating the respective signaling pathways *in vitro*. This demonstrated that cofilin1 deficient thymocytes still have the intrinsic capacity to differentiate once the appropriate signals are provided.

Our data also excluded a number of rather trivial explanations for the observed differentiation block. Previously described functions of cofilin1 in apoptosis (Chua et al., 2003; Wabnitz et al., 2010), cell proliferation (Eibert et al., 2004; Ohashi, 2015), and receptor trafficking (Salvarezza et al., 2009; von Blume et al., 2011) seem to be rather cell specific functions, but not relevant in thymocyte development. In addition, it is important to note that the function of cofilin1 is clearly cell autonomous in thymocytes. As mentioned, our CD4-cre mouse model allows a small percentage of thymocytes to escape deletion. These escaper cells express cofilin1, developed into mature CD4SP or CD8SP cells, and populated peripheral lymphatic tissues. This finding excludes epiphenomena due to tissue architecture or any other secondary effects. In addition, unpublished data from our group on the deletion of cofilin1 in mTECs using a K14-cre driver line, showed no impairment in thymocyte development (Gurniak&Witke, unpublished observation).

In Cof1$^{fl/fl,CD4cre}$ mutant mice the block of α,β thymocyte differentiation had a number of physiological consequences, such as the severe lack of peripheral T cells and the relative increase of B cells in secondary lymphatic compartments. Alterations in the B cell compartments had been observed before (Molina et al., 1992; Negishi et al., 1995), however in our case of Cof1$^{fl/fl,CD4cre}$ mutant mice the absolute number of B cells in secondary lymphatic tissues was unchanged (Suppl. Fig. E).

In this context we should note that heterozygous cofilin1 mutants (Cof1$^{wt/fl,CD4cre}$), expressing 50% of normal cofilin1 protein levels showed no impairment in T cell development or alterations in any T cell subset we have analysed.

Control of cofilin1 activity is a powerful mean to regulate T cell differentiation. In the physiological context, cofilin1 is regulated by different mechanisms (Bernstein and

Bamburg, 2010; Van Troys et al., 2008). One control mechanism is phosphorylation of Ser3, which is shutting off activity while dephosphorylation activates cofilin1 (Nagaoka et al., 1996). Studies have shown dephosphorylation of cofilin1 after T cell stimulation (Samstag et al., 1992), however whether phosphorylation is relevant in thymocytes during the initial F-actin burst has not been addressed yet. In a recent study it was shown that expression of a GFP-cofilin1 variant in DN cells that cannot be phosphorylated is blocking T cell development at the DN stage (Seeland et al., 2018). In this model the GFP-cofilin1 variant apparently has a dominant effect in DN cells, leading to the loss of 99% of thymocytes, while in our knockout model normal numbers of DP cells were observed. In addition, the Seeland et al. model showed that γ,δ T cells were present in normal numbers. In contrast, in our knockout model we observed an upregulation of γ,δ T cell numbers as an intriguing epiphenomenon since in these γ,δ T cells the CD4-cre mediated deletion occurs at only very low levels (Suppl. Fig. C,D).

Our results on cofilin1 function in thymocyte differentiation is distinct from the numerous studies on the role of cofilin1 in mature T cells or other cell types. Our approach does indeed not allow to draw any conclusions on coflin1 function in mature T cells upon stimulation and cell activity (Eibert et al., 2004; Lee et al., 2000).

In conclusion, we propose a new function of cofilin1 in regulating the coordinated migration and adhesion of thymocytes during positive selection and differentiation into single positive T cells.

Material and Methods

Mouse lines. The generation of the Cofilin1 conditional mouse line ($Cof1^{fl/fl}$) was described by Gurniak et al., 2005 and the respective alleles are illustrated in Fig. 1C. $Cof1^{fl/lfl}$ mice were crossed to a transgenic mouse line which expresses Cre recombinase under the CD4 promoter (Wolfer et al., 2001). Animals homozygous for the Cofilin1 flox-allele and heterozygous for the CD4-cre allele ($Cof1^{fl/fl,CD4cre}$) were used for experiments. Unless specified differently, control mice were either littermates homozygous for the cofilin1 flox-allele ($Cof1^{fl/fl}$) or mice wildtype for cofilin1 and heterozygous for CD4-cre ($Cof1^{wt/wt,CD4cre}$). The Rosa26-Stop-YFP reporter line carries a floxed 'Stop cassette' in the ubiquitously expressed Rosa26 locus (Srinivas et al., 2001). Upon Cre-mediated deletion of the 'Stop cassette' YFP expression can be

observed. Unless specified otherwise, the n given in the figure legends refers to the biological n, meaning the number of animals used in independent experiments. Genotyping was performed by PCR using gene and mutation specific primers. Animal housing, breeding, and procedures were carried out according to EU regulations and permission granted by local authorities in Italy and Germany ('Decreto n. 19/2005-B' and AZ 81-02.04.2019.A233).

Cell preparation and sorting. Tissues were obtained from adult 6 weeks to 3 months old animals and single cell suspensions were prepared from thymus in RPMI 1640 medium without phenol red. For Southern- and Western-blot analyses of peripheral T cells $CD4^+$ cells from spleen were sorted using magnetic beads according to the manufacturer's protocol (Miltenyi Biotec). As judged by FACS staining using CD4-PerCP and CD8-FITC the sorted $CD4^+$ cell populations were more than 90% pure.

Flow cytometry. Up to four-color FACS staining was performed as described by Gurniak and Witke, 2007. Briefly, single cell suspensions were filtered (30µm Filcons) and stained with the corresponding antibodies in FACS buffer (0.5% FCS, 2mM EDTA in PBS) for 15 to 30min on ice, washed two times with FACS buffer and data were acquired on an Accuri C6 (Becton Dickinson (BD)). *Actin measurements*: To determine G- and F-actin levels by DNaseI and phalloidin staining, cells were fixed in 4% PFA/PBS for 10min washed with PBS and permeabilized for 15min with 0.1% Triton X-100/PBS, both incubations at RT. *Apoptosis staining:* For apoptotic and dead cells the Annexin V-FITC Apoptosis Detection Kit (BD) was used in combination with propidium iodide, staining for CD4-PerCP and CD8-APC was performed simultaneously. For intracellular staining of active caspase 3, live thymocytes were first stained for CD4 and CD8, then fixed with 4% PFA/PBS, permeabilized by 0.1% TritonX-100/PBS, and stained with Alexa-488 conjugated anti-active caspase 3 (Cell Signaling Technology). Incubation steps with fluorophores were carried out on ice, and reagents were diluted in FACS buffer. *Fluorescent labels:* Antibodies from eBioscience: FITC conjugated anti-CD4, anti-CD8, anti-TCRß; PerCP$_{efluor710®}$ conjugated anti-CD4; allophycocyanin (APC) conjugated anti-TCRß, anti-CD8, anti-CD184, anti-CD197, anti-CD199. Reagents from BD: FITC conjugated anti-CD8; Phycoerythrin (PE) conjugated anti-CD19, anti-CD69 and anti-TCRß; PerCP conjugated anti-CD19 and anti-CD8; APC conjugated anti-CD19; 7-aminoactinomycin D (7-AAD). Reagents from Molecular Probes™: Alexa-680 conjugated phalloidin and Alexa-488 conjugated DNaseI.

Thymocyte culture and treatments. For *in vitro* differentiation of thymocytes as described by (Cibotti et al., 1997), 3cm polystyrene Petri dishes (Greiner Bio-One) were coated for 3h at room temperature with TCRß and CD2 antibodies (eBioscience) at a concentration of 5µg/ml in 50mM Tris/HCl pH 9.5. 1 x 10^7 thymocytes were cultured at 37°C, 5% CO_2 in 1ml RPMI 1640 medium containing 1.76µM 2-mercaptoethanol and 10% heat inactivated FCS, which had been depleted of endogenous steroids by charcoal and dextran. After 18h cells were washed and transferred for recovery culture onto uncoated petri dishes for additional 16h, before FACS analysis. *Pronase treatment:* The CD4/CD8 receptor re-expression assay was essentially performed as described in (Ohoka et al., 1996; Punt et al., 1996). Briefly, thymocytes were washed three times with PBS and 2 x 10^6 cells/ml were treated two times with 0.02% Pronase (Calbiochem) and 100µg/ml DNaseI (Promega) diluted in PBS for 15min at 37°C. To quench the reaction 10% FCS was added, cells were washed tree times with RPMI 1640 medium. For receptor recovery cells were incubated in RPMI 1640 medium for 1h, 6h and 14h at 37°C, 5% CO_2 or at 4°C, before staining and FACS analysis.

Cell cycle analysis and proliferation assay. The cell cycle kit by BD was used to analyse the DNA content of total thymocytes. After fixation, RNase treatment and propidium iodide staining single cells were acquired by flow cytometry. To determine the proliferation rate of total thymocytes 5x10^4 cells were seeded into 96 well plates and incubated for 0, 24, 48 and 72 hours with or without 10ng/ml PMA and 400nM Ionomycin in RPMI 1640 medium at 37°C, 5% CO_2. After centrifugation and removal of medium plates were frozen at -80°C. Cell number was determined by staining of DNA with Cyquant™ (Thermo Fisher Scientific) and fluorometric analysis.

Adhesion, Spreading and migration assays. The *adhesion assay* on ICAM-1 was performed as outlined by Quast et al., 2009 and Boehm et al., 2003. For efficient coating of ICAM-1 to the plastic surface a precoating of human IgG FCγ monoclonal antibody (Dianova) followed by binding of recombinant mouse ICAM-1-FC chimera (R&D Systems) was used. As a control, we kept an ICAM-1 uncoated ring area on the plastic surface. Thymocytes were stimulated with 400ng/ml SDF-1α (PeproTech) for 60min and cells were then allowed to attach for 1h. Unbound cells were rinsed off with HBSS until the outer uncoated ring area was devoid of cells. Adherent cells were then fixed with 4% PFA/PBS for 10min and counted manually in seven random fields of view

using a 10x phase contrast objective (Nikon) with a fully automated inverted microscope (Keyence). To determine spreading the number of extended cells were counted from phase contrast images. Statistics were performed by a two-tailed independent T-test and with SigmaPlot® 12 (Systat Software, Inc.) using one-way Anova.

Transwell assay: Two dimensional migration of thymocytes was measured by transwell migration using inserts with a pore size of 5µm (Corning Costar) as described by Phee et al., 2010 and Shiow et al., 2008. Single cell suspensions were preincubated for 1h in migration medium (10mM HEPES pH 7.2, 100U/ml penicillin/streptomycin, 0.5% (v/v) BSA in RPMI 1640) at 37°C, 5% CO_2, subsequently 3 x 10^5 cells were transferred to the top chamber of the respective transwell plates. Assays were set up in duplicates; the bottom chamber contained plain migration medium or one of the chemokines either SDF-1α (400ng/ml) or CCL25 (2.5µg/ml) (both from PeproTech) diluted in migration medium. After an incubation time of 5h at 37°C, 5% CO_2 cells were collected from the bottom well and stained with antibodies directed against CD4-PerCP, CD8-PE and TCRß-APC and analysed by flow cytometry. The receptors for the chemokines SDF-1α and CCL25 were stained with the antibodies CD184-APC and CD199-APC, respectively.

3D migration in collagen gel: For the analysis of thymocyte motility in 3D, migration assays were performed in polymerised rat tail collagen-I (Gibco® INVITROGEN) according to the protocol of Friedl et al., 1998 and Quast et al., 2009. On ice collagen-I was titrated with 0.1N NaOH and mixed with 10x MEM (Gibco® INVITROGEN) and the chemokines SDF-1α (400ng/ml) or CCL25 (2.5µg/ml) (PeproTech). 3 x 10^5 thymocytes in migration medium were carefully mixed with 100µl collagen solution, resulting in a final collagen-I concentration of 3mg/ml. Collagen-thymocyte mixtures were placed in custom-built chemotaxis chambers and incubated for 60min at 37°C, 5% CO_2 to allow collagen polymerisation and cell recovery. Time-lapse imaging was conducted using a fully automated inverted microscope (Keyence) equipped with a 10x phase-contrast objective (Nikon) and a climate chamber (37°C; 5% CO_2). Time-lapse images were recorded for 8h at 90s intervals; control and mutant thymocytes were simultaneously acquired at different coordinates. The ImageJ 1.47q software (NIH) and the 'Manual Tracking' plug-in (NIH) were used to track cell paths. The 'Chemotaxis and Migration Tool' Version 1.01 plug-in (ibidi Integrated BioDiagnostics) were employed for plotting

cell tracks and for the measurements of velocity and distance. Movies were processed using ImageJ 1.47q. Statistics were performed by SigmaPlot® 12 (Systat Software, Inc.) by Mann-Whitney test, and by a two tailed independent T-test.

Histology. Hematoxylin/Eosin (H&E) staining was carried out on 8µm cryo sections; after fixation with 4% PFA/PBS slides were incubated in 0.05% Eosin (Sigma-Aldrich) and 20% Hematoxylin (Merck Millipore). Area measurements of thymic regions were performed manually on H&E stained sections using the area measurement plug-in of the Keyence BZ-II analyser software (version 1.41)**.**

Western blot analysis. Total protein lysates were prepared from single cell suspensions boiled in SDS sample buffer (22mM Tris/HCl, pH 6.8, 4% glycerol, 0.8% SDS, 1.6% 2-mercaptoethanol, bromophenol blue). The samples were separated by SDS-PAGE, transferred to Immobilon-P membrane (Merck Millipore) and probed with antibodies. Signals were developed using ECL and recorded digitally on a LAS4000 (General Electric). Equal loading was verified by Coomassie staining and GAPDH as internal standard. *Antibodies used*: mouse anti-GAPDH (Merck); rabbit anti-cofilin1, rabbit anti-cofilin2, mouse anti-ADF (Gurniak et al., 2014); rabbit anti-gelsolin (Witke et al., 1995), rabbit anti-CapG (Witke et al., 2001), anti-actin (MP Biomedicals), horseradish peroxidase conjugated anti-mouse, anti-rabbit and anti-rat IgG (Jackson Immuno Research).

Southern blotting. CD4-cre mediated deletion of the floxed Cofilin1 alleles were analysed by PCR and Southern blot as described by Gurniak et al., 2005 using genomic DNA isolated from single cell suspensions and tail biopsies.

Acknowledgements

We thank Melanie Jokwitz and Gabi Matern for technical assistance, the EMBL Monterotondo for support during the course of the experiments, and the funding agencies for support to WW (SFB 704, SPP 1464).

Competing interests: No competing interests are declared.

Author contribution: Conceptualization: W.W., C.B.G; Experiments performed: A.S., C.B.G., F.J.; manuscript writing: W.W., C.B.G., A.S., F.J.; funding acquisition: W.W

Funding: This study was supported by grants from the DFG (Deutsche Forschungsgemeinschaft) as part of the Collaborative Research Centre 'SFB 704', and the Priority Programme 'SPP 1464'.

References

Anderson, G. and Jenkinson, E. J. (2001). Lymphostromal interactions in thymic development and function. *Nat. Rev. Immunol.* **1**, 31–40.

Bellenchi, G. C., Gurniak, C. B., Perlas, E., Middei, S., Ammassari-Teule, M. and Witke, W. (2007). N-cofilin is associated with neuronal migration disorders and cell cycle control in the cerebral cortex. *Genes Dev.* **21**, 2347–2357.

Bernstein, B. W. and Bamburg, J. R. (2010). ADF/Cofilin: A functional node in cell biology. *Trends Cell Biol.* **20**, 187–195.

Billadeau, D. D., Nolz, J. C. and Gomez, T. S. (2007). Regulation of T-cell activation by the cytoskeleton. *Nat. Rev. Immunol.* **7**, 131–143.

Boehm, T., Hofer, S., Winklehner, P., Kellersch, B., Geiger, C., Trockenbacher, A., Neyer, S., Fiegl, H., Ebner, S., Ivarsson, L., et al. (2003). Attenuation of cell adhesion in lymphocytes is regulated by CYTIP, a protein which mediates signal complex sequestration. *EMBO J.* **22**, 1014–24.

Brakebusch, C. and Fässler, R. (2003). The integrin-actin connection, an eternal love affair. *EMBO J.* **22**, 2324–2333.

Bunnell, S. C., Kapoor, V., Trible, R. P., Zhang, W., Samelson, L. E., Carolina, N. and Sos, R. (2001). T Cell Receptor – Induced Spreading : A Role for the Signal Transduction Adaptor LAT. *Immunity* **14**, 315–329.

Carlier, M. F., Laurent, V., Santolini, J., Melki, R., Didry, D., Xia, G. X., Hong, Y., Chua, N. H. and Pantaloni, D. (1997). Actin depolymerizing factor (ADF/cofilin) enhances the rate of filament turnover: implication in actin-based motility. *J. Cell Biol.* **136**, 1307–22.

Ceredig, R. and Rolink, T. (2002). A positive look at double-negative thymocytes. *Nat. Rev. Immunol.* **2**, 888–896.

Chua, B. T., Volbracht, C., Tan, K. O., Li, R., Yu, V. C. and Li, P. (2003). Mitochondrial translocation of cofilin is an early step in apoptosis induction. *Nat. Cell Biol.* **5**, 1083–1089.

Cibotti, R., Punt, J. A., Dash, K. S., Sharrow, S. O. and Singer, A. (1997). Surface molecules that drive T cell development in vitro in the absence of thymic epithelium and in the absence of lineage-specific signals. *Immunity* **6**, 245–255.

Cleverley, S., Henning, S. and Cantrell, D. (1999). Inhibition of Rho at different stages of thymocyte development gives different perspectives on Rho function. *Curr. Biol.* **9**, 657–660.

Costello, P. S., Cleverley, S. C., Galandrini, R., Henning, S. W. and Cantrell, D. A. (2000). The Gtpase Rho Controls a P53-Dependent Survival Checkpoint during Thymopoiesis. *J. Exp. Med.* **192**, 77–86.

Delon, J., Bercovici, N., Liblau, R. and Trautmann, A. (1998). Imaging antigen recognition by naive CD4+ T cells: Compulsory cytoskeletal alterations for the triggering of an intracellular calcium response. *Eur. J. Immunol.* **28**, 716–729.

Dustin, M. L. and Cooper, J. A. (2000). The immunological synapse and the actin cytoskeleton: Molecular hardware for T cell signaling. *Nat. Immunol.* **1**, 23–29.

Eibert, S. M., Lee, K.-H., Pipkorn, R., Sester, U., Wabnitz, G. H., Giese, T., Meuer, S. C. and Samstag, Y. (2004). Cofilin peptide homologs interfere with immunological synapse formation and T cell activation. *Proc. Natl. Acad. Sci.* **101**, 1957–1962.

Fine, J. A. Y. S. and Kruisbeek, A. D. A. M. (1991). The role of LFA-1 / ICAM-1 interactions during murine T lymphocyte development . J S Fine and A M Kruisbeek Information about subscribing to The Journal of Immunology is online at : THE ROLE OF LFA-l / ICAM-l INTERACTIONS DURING MURINE LYMPHOCYTE DEVELOPM. *J. Immunol.* **147**, 2852–2859.

Flynn, K. C., Neukirchen, D., Tahirovic, S., Garvalov, B. K., Meyn, L., Bradke, F., Hellal, F., Dupraz, S., Stern, S., Jacob, S., et al. (2012). ADF/Cofilin-Mediated Actin Retrograde Flow Directs Neurite Formation in the Developing Brain. *Neuron* **76**, 1091–1107.

Friedl, P., Entschladen, F., Conrad, C., Niggemann, B. and Zänker, K. S. (1998). CD4+ T lymphocytes migrating in three-dimensional collagen lattices lack focal adhesions and utilize beta1 integrin-independent strategies for polarization, interaction with collagen fibers and locomotion. *Eur. J. Immunol.* **28**, 2331–43.

Friedl, P., Borgmann, S. and Bröcker, E. B. (2001). Amoeboid leukocyte crawling through extracellular matrix: lessons from the Dictyostelium paradigm of cell movement. *J. Leukoc. Biol.* **70**, 491–509.

Galandrini, R., Henning, S. W. and Cantrell, D. A. (1997). Different functions of the GTpase Rho in prothymocytes and late pre-T cells. *Immunity* **7**, 163–174.

Ghosh, M., Song, X., Mouneimne, G., Sidani, M., Lawrence, D. S. and Condeelis, J. S. (2004). Cofilin promotes actin polymerization and defines the direction of cell motility. *Science* **304**, 743–6.

Godfrey, D. I., Kennedy, J., Suda, T. and Zlotnik, A. (1993). A developmental pathway involving four phenotypically and functionally distinct subsets of CD3-CD4-CD8- triple-negative adult mouse thymocytes defined by CD44 and CD25 expression. *J. Immunol.* **150**, 4244–52.

Gomez, M., Kioussis, D. and Cantrell, D. A. (2001). The GTPase Rac-1 controls cell fate in the thymus by diverting thymocytes from positive to negative selection. *Immunity* **15**, 703–713.

Guidos, C. J., Danska, J. S., Fathman, C. G. and Weissman, I. L. (1990). T cell receptor-mediated negative selection of autoreactive T lymphocyte precursors occurs after commitment to the CD4 or CD8 lineages. *J. Exp. Med.* **172**, 835–45.

Gurniak, C. B. and Witke, W. (2007). HuGE, a novel GFP-actin-expressing mouse line for studying cytoskeletal dynamics. *Eur. J. Cell Biol.* **86**, 3–12.

Gurniak, C. B., Perlas, E. and Witke, W. (2005). The actin depolymerizing factor n-cofilin is essential for neural tube morphogenesis and neural crest cell migration. *Dev. Biol.* **278**, 231–241.

Gurniak, C. B., Chevessier, F., Jokwitz, M., Jönsson, F., Perlas, E., Richter, H., Matern, G., Boyl, P. P., Chaponnier, C., Fürst, D., et al. (2014). Severe protein aggregate myopathy in a knockout mouse model points to an essential role of cofilin2 in sarcomeric actin exchange and muscle maintenance. *Eur. J. Cell Biol.* **93**, 252–66.

Henning, S. (1997). The small GTPase Rho has a critical regulatory role in thymic development. *Immunol. Lett.* **56**, 9.

Jameson, S. C. and Bevan, M. J. (1998). T-cell selection. *Curr. Opin. Immunol.* **10**, 214–219.

Jönsson, F., Gurniak, C. B., Fleischer, B., Kirfel, G. and Witke, W. (2012). Immunological responses and actin dynamics in macrophages are controlled by N-cofilin but are independent from ADF. *PLoS One* **7**, 1–12.

Kato, A., Kurita, S., Hayashi, A., Kaji, N., Ohashi, K. and Mizuno, K. (2008). Critical roles of actin-interacting protein 1 in cytokinesis and chemotactic migration of mammalian cells. *Biochem. J.* **414**, 261–270.

Krause, M., Sechi, A. S., Konradt, M., Monner, D., Gertler, F. B. and Wehland, J. (2000). Fyn-binding protein (Fyb)/SLP-76-associated protein (SLAP), ena/vasodilator-stimulated phosphoprotein (VASP) proteins and the Arp2/3 complex link T cell receptor (TCR) signaling to the actin cytoskeleton. *J. Cell Biol.* **149**, 181–194.

Ladi, E., Yin, X., Chtanova, T. and Robey, E. A. (2006). Thymic microenvironments for T cell differentiation and selection. *Nat. Immunol.* **7**, 338–343.

Ladi, E., Schwickert, T. A., Chtanova, T., Chen, Y., Herzmark, P., Yin, X., Aaron, H., Chan, S. W., Lipp, M., Roysam, B., et al. (2008). Thymocyte-Dendritic Cell Interactions near Sources of CCR7 Ligands in the Thymic Cortex. *J. Immunol.* **181**, 7014–7023.

Lancaster, J. N., Li, Y. and Ehrlich, L. I. R. (2018). Chemokine-Mediated Choreography of Thymocyte Development and Selection. *Trends Immunol.* **39**, 86–98.

Le Borgne, M., Ladi, E., Dzhagalov, I., Herzmark, P., Liao, Y. F., Chakraborty, A. K. and Robey, E. A. (2009). The impact of negative selection on thymocyte migration in the medulla. *Nat. Immunol.* **10**, 823–830.

Lee, K. H., Meuer, S. C. and Samstag, Y. (2000). Cofilin: A missing link between T cell co-stimulation and rearrangement of the actin cytoskeleton. *Eur. J. Immunol.* **30**, 892–899.

Lind, E. F., Prockop, S. E., Porritt, H. E. and Petrie, H. T. (2001). Mapping Precursor Movement through the Postnatal Thymus Reveals Specific Microenvironments Supporting Defined Stages of Early Lymphoid Development. *J. Exp. Med.* **194**, 127–134.

Love, P. E. and Bhandoola, A. (2011). Signal integration and crosstalk during thymocyte migration and emigration. *Nat. Rev. Immunol.* **11**, 469–477.

Lub, M., van Kooyk, Y., van Vliet, S. J. and Figdor, C. G. (1997). Dual role of the actin cytoskeleton in regulating cell adhesion mediated by the integrin lymphocyte function-associated molecule-1. *Mol. Biol. Cell* **8**, 341–351.

Maciver, S. K., Zot, H. G. and Pollard, T. D. (1991). Characterization of actin filament severing by actophorin from Acanthamoeba castellanii. *J. Cell Biol.* **115**, 1611–20.

Malissen, B. and Malissen, M. (1996). Functions of TCR and pre-TCR subunits: lessons from gene ablation. *Curr. Opin. Immunol.* **8**, 383–93.

Matsui, S., Adachi, R., Kusui, K., Yamaguchi, T., Kasahara, T., Hayakawa, T. and Suzuki, K. (2001). U73122 inhibits the dephosphorylation and translocation of cofilin in activated macrophage-like U937 cells. *Cell. Signal.* **13**, 17–22.

McGough, A., Pope, B., Chiu, W. and Weeds, A. (1997). Cofilin changes the twist of F-actin: implications for actin filament dynamics and cellular function. *J. Cell Biol.* **138**, 771–81.

McRobbie, S. J. and Newell, P. C. (1983). Changes in actin associated with the cytoskeleton following chemotactic stimulation of dictyostelium discoideum. *Biochem. Biophys. Res. Commun.* **115**, 351–9.

Mitnacht, R., Bischof, A., Torres-Nagel, N. and Hünig, T. (1998). Opposite CD4/CD8 lineage decisions of CD4+8+ mouse and rat thymocytes to equivalent triggering signals: correlation with thymic expression of a truncated CD8 alpha chain in mice but not rats. *J. Immunol.* **160**, 700–7.

Molina, T. J., Kishihara, K., Siderovski, D. P., van Ewijk, W., Narendran, A., Timms, E., Wakeham, A., Paige, C. J., Hartmann, K. U. and Veillette, A. (1992). Profound block in thymocyte development in mice lacking p56lck. *Nature* **357**, 161–4.

Monks, C. R. F., Freiberg, B. A., Kupfer, H., Sciaky, N. and Kupfer, A. (1998). Three-dimensional segregation of supramolecular activation clusters in T cells. *Nature* **395**, 82–86.

Nagaoka, R., Abe, H. and Obinata, T. (1996). Site-directed mutagenesis of the phosphorylation site of cofilin: Its role in cofilin-actin interaction and cytoplasmic localization. *Cell Motil. Cytoskeleton* **35**, 200–209.

Nakashima, K., Sato, N., Nakagaki, T., Abe, H., Ono, S. and Obinata, T. (2005). Two mouse cofilin isoforms, muscle-type (MCF) and non-muscle type (NMCF), interact with F-actin with different efficiencies. *J. Biochem.* **138**, 519–526.

Negishi, I., Motoyama, N., Nakayama, K., Nakayama, K., Senju, S., Hatakeyama, S., Zhang, Q., Chan, A. C. and Loh, D. Y. (1995). Essential role for ZAP-70 in both positive and negative selection of thymocytes. *Nature* **376**, 435–8.

Nishita, M., Tomizawa, C., Yamamoto, M., Horita, Y., Ohashi, K. and Mizuno, K. (2005). Spatial and temporal regulation of cofilin activity by LIM kinase and Slingshot is critical for directional cell migration. *J. Cell Biol.* **171**, 349–359.

Nolz, J. C., Gomez, T. S., Zhu, P., Li, S., Medeiros, R. B., Shimizu, Y., Burkhardt, J. K., Freedman, B. D. and Billadeau, D. D. (2006). The WAVE2 complex regulates actin cytoskeletal reorganization and CRAC-mediated calcium entry during T cell activation. *Curr. Biol.* **16**, 24–34.

Norment, A. M. and Bevan, M. J. (2000). Role of chemokines in thymocyte development. *Semin. Immunol.* **12**, 445–455.

Ohashi, K. (2015). Roles of cofilin in development and its mechanisms of regulation. *Dev. Growth Differ.* **57**, 275–290.

Ohoka, Y., Kuwata, T., Tozawa, Y., Zhao, Y., Mukai, M., Motegi, Y., Suzuki, R., Yokoyama, M. and Iwata, M. (1996). In vitro differentiation and commitment of CD4 + CD8 + thymocytes to the CD4 lineage without TCR engagement. *Int. Immunol.* **8**, 297–306.

Peled, A., Kollet, O., Ponomaryov, T., Petit, I., Franitza, S., Grabovsky, V., Slav, M. M., Nagler, A., Lider, O., Alon, R., et al. (2000). The chemokine SDF-1 activates the integrins LFA-1, VLA-4, and VLA-5 on immature human CD34(+) cells: role in transendothelial/stromal migration and engraftment of NOD/SCID mice. *Blood* **95**, 3289–96.

Penninger, J. M. and Crabtree, G. R. (1999). The actin cytoskeleton and lymphocyte activation. *Cell* **96**, 9–12.

Phee, H., Dzhagalov, I., Mollenauer, M., Wang, Y., Irvine, D. J., Robey, E. and Weiss, A. (2010). Regulation of thymocyte positive selection and motility by GIT2. *Nat. Immunol.* **11**, 503–511.

Phillips, D. R., Jennings, L. K. and Edwards, H. H. (1980). Identification of membrane proteins mediating the interaction of human platelets. *J. Cell Biol.* **86**, 77–86.

Philpott, K. L., Viney, J. L., Kay, G., Rastan, S., Gardiner, E. M., Chae, S., Hayday, A. C. and Owen, M. J. (1992). Lymphoid development in mice congenitally lacking T cell receptor alpha beta-expressing cells. *Science* **256**, 1448–52.

Porritt, H. E., Gordon, K. and Petrie, H. T. (2003). Kinetics of Steady-state Differentiation and Mapping of Intrathymic-signaling Environments by Stem Cell Transplantation in Nonirradiated Mice. *J. Exp. Med.* **198**, 957–962.

Punt, J. A., Suzuki, H., Granger, L. G., Sharrow, S. O. and Singer, A. (1996). Lineage commitment in the thymus: only the most differentiated (TCRhibcl-2hi) subset of CD4+CD8+ thymocytes has selectively terminated CD4 or CD8 synthesis. *J. Exp. Med.* **184**, 2091–9.

Quast, T., Tappertzhofen, B., Schild, C., Grell, J., Czeloth, N., Förster, R., Alon, R., Fraemohs, L., Dreck, K., Weber, C., et al. (2009). Cytohesin-1 controls the activation of RhoA and modulates integrin-dependent adhesion and migration of dendritic cells. *Blood* **113**, 5801–5810.

Rust, M. B., Gurniak, C. B., Renner, M., Vara, H., Morando, L., Görlich, A., Sassoè-Pognetto, M., Banchaabouchi, M. Al, Giustetto, M., Triller, A., et al. (2010). Learning, AMPA receptor mobility and synaptic plasticity depend on n-cofilin-mediated actin dynamics. *EMBO J.* **29**, 1889–1902.

Salvarezza, S. B., Deborde, S., Schreiner, R., Campagne, F., Kessels, M. M., Qualmann, B., Caceres, A., Kreitzer, G. and Rodriguez-Boulan, E. (2009). LIM kinase 1 and cofilin regulate actin filament population required for dynamin-dependent apical carrier fission from the trans-Golgi network. *Mol. Biol. Cell* **20**, 438–51.

Samstag, Y., Henning, S. W., Bader, A. and Meuer, S. C. (1992). Dephosphorylation of pp19: A common second signal for human T cell activation mediated through different accessory molecules. *Int. Immunol.* **4**, 1255–1262.

Samstag, Y., Eibert, S. M., Klemke, M. and Wabnitz, G. H. (2003). Actin cytoskeletal dynamics in T lymphocyte activation and migration of the immunological synapse at the interface be-. *J. Leukoc. Biol.* **73**, 30–48.

Savino, W., Mendes-da-Cruz, D. A., Smaniotto, S., Silva-Monteiro, E. and Villa-Verde, D. M. S. (2004). Molecular mechanisms governing thymocyte migration: combined role of chemokines and extracellular matrix. *J. Leukoc. Biol.* **75**, 951–961.

Sebzda, E., Mariathasan, S., Ohteki, T., Jones, R., Bachmann, M. F. and Ohashi, P. S. (1999). Selection of the T Cell Repertoire. *Annu. Rev. Immunol.* **17**, 829–874.

Sechi, A. S. and Wehland, J. (2004). Interplay between TCR signalling and actin cytoskeleton dynamics. *Trends Immunol.* **25**, 257–265.

Seeland, I., Xiong, Y., Orlik, C., Deibel, D., Prokosch, S., Küblbeck, G., Jahraus, B., De Stefano, D., Moos, S., Kurschus, F. C., et al. (2018). The actin remodeling protein cofilin is crucial for thymic αβ but not γδ T-cell development. *PLoS Biol.* **16**, 1–21.

Shiow, L. R., Roadcap, D. W., Paris, K., Watson, S. R., Grigorova, I. L., Lebet, T., An, J., Xu, Y., Jenne, C. N., Föger, N., et al. (2008). The actin regulator coronin 1A is mutant in a thymic egress-deficient mouse strain and in a patient with severe combined immunodeficiency. *Nat. Immunol.* **9**, 1307–1315.

Srinivas, S., Watanabe, T., Lin, C. S., William, C. M., Tanabe, Y., Jessell, T. M. and Costantini, F. (2001). Cre reporter strains produced by targeted insertion of EYFP and ECFP into the ROSA26 locus. *BMC Dev. Biol.* **1**, 4.

Stossel, T. P. (1993). On the crawling of animal cells. *Science* **260**, 1086–94.

Stradal, T. E. B., Pusch, R. and Kliche, S. (2006). Molecular regulation of cytoskeletal rearrangements during T cell signalling. *Results Probl. Cell Differ.* **43**, 219–44.

Swat, W., Dessing, M., von Boehmer, H. and Kisielow, P. (1993). CD69 expression during selection and maturation of CD4+8+ thymocytes. *Eur. J. Immunol.* **23**, 739–46.

Takahama, Y. (2006). Journey through the thymus: Stromal guides for T-cell development and selection. *Nat. Rev. Immunol.* **6**, 127–135.

Uehara, S., Grinberg, A., Farber, J. M. and Love, P. E. (2002a). A Role for CCR9 in T Lymphocyte Development and Migration. *J. Immunol.* **168**, 2811–2819.

Uehara, S., Song, K., Farber, J. M. and Love, P. E. (2002b). Characterization of CCR9 Expression and CCL25/Thymus-Expressed Chemokine Responsiveness During T Cell Development: CD3 high CD69 + Thymocytes and γδTCR + Thymocytes Preferentially Respond to CCL25 . *J. Immunol.* **168**, 134–142.

Van Troys, M., Huyck, L., Leyman, S., Dhaese, S., Vandekerkhove, J. and Ampe, C. (2008). Ins and outs of ADF/cofilin activity and regulation. *Eur. J. Cell Biol.* **87**, 649–667.

Vartiainen, M. K. (2002). The Three Mouse Actin-depolymerizing Factor/Cofilins Evolved to Fulfill Cell-Type-specific Requirements for Actin Dynamics. *Mol. Biol. Cell* **13**, 183–194.

von Blume, J., Alleaume, A. M., Cantero-Recasens, G., Curwin, A., Carreras-Sureda, A., Zimmermann, T., van Galen, J., Wakana, Y., Valverde, M. A. and Malhotra, V. (2011). ADF/cofilin regulates secretory cargo sorting at the TGN via the Ca2+ ATPase SPCA1. *Dev. Cell* **20**, 652–662.

Von Boehmer, H., Aifantis, I., Feinberg, J., Lechner, O., Saint-Ruf, C., Walter, U., Buer, J. and Azogui, O. (1999). Pleiotropic changes controlled by the pre-T-cell receptor. *Curr. Opin. Immunol.* **11**, 135–142.

Wabnitz, G. H., Goursot, C., Jahraus, B., Kirchgessner, H., Hellwig, A., Klemke, M., Konstandin, M. H. and Samstag, Y. (2010). Mitochondrial translocation of oxidized cofilin induces caspase-independent necrotic-like programmed cell death of T cells. *Cell Death Dis.* **1**, 1–12.

Watts, R. G. and Howard, T. H. (1993). Mechanisms for actin reorganization in chemotactic factor-activated polymorphonuclear leukocytes. *Blood* **81**, 2750–7.

Witke, W., Sharpe, A. H., Hartwig, J. H., Azuma, T., Stossel, T. P. and Kwiatkowski, D. J. (1995). Hemostatic, inflammatory, and fibroblast responses are blunted in mice lacking gelsolin. *Cell* **81**, 41–51.

Witke, W., Li, W., Kwiatkowski, D. J. and Southwick, F. S. (2001). Comparisons of CapG and gelsolin-null macrophages: Demonstration of a unique role for CapG in receptor-mediated ruffling, phagocytosis, and vesicle rocketing. *J. Cell Biol.* **154**, 775–784.

Witt, C. M., Raychaudhuri, S., Schaefer, B., Chakraborty, A. K. and Robey, E. A. (2005). Directed migration of positively selected thymocytes visualized in real time. *PLoS Biol.* **3**, 1062–1069.

Wolfer, A., Bakker, T., Wilson, A., Nicolas, M., Ioannidis, V., Littman, D. R., Wilson, C. B., Held, W., MacDonald, H. R. and Radtke, F. (2001). Inactivation of Notch1 in immature thymocytes does not perturb CD4 or CD8 T cell development. *Nat. Immunol.* **2**, 235–241.

Wurbel, M. A., Philippe, J. M., Nguyen, C., Victorero, G., Freeman, T., Wooding, P., Miazek, A., Mattei, M. G., Malissen, M., Jordan, B. R., et al. (2000). The chemokine TECK is expressed by thymic and intestinal epithelial cells and attracts double- and single-positive thymocytes expressing the TECK receptor CCR9. *Eur. J. Immunol.* **30**, 262–71.

Xu, X., Guo, J., Vorster, P. J. and Wu, Y. (2012). Involvement of LIM kinase 1 in actin polarization in human CD4 T cells. *Commun. Integr. Biol.* **5**, 381–383.

Yamashita, I., Nagata, T., Tada, T. and Nakayama, T. (1993). CD69 cell surface expression identifies developing thymocytes which audition for T cell antigen receptor-mediated positive selection. *Int. Immunol.* **5**, 1139–1150.

Zaitseva, M. B., Lee, S., Peden, K. W. C., Golding, H., Rabin, R. L., Farber, J. M., Tiffany, H. L. and Murphy, P. M. (1998). CXCR4 and CCR5 on human thymocytes: Biological function and role in HIV- 1 infection. *J. Immunol.* **161**, 3103–3113.

Zhang, J., Shi, F., Badour, K., Deng, Y., McGavin, M. K. H. and Siminovitch, K. A. (2002). WASp verprolin homology, cofilin homology, and acidic region domain-mediated actin polymerization is required for T cell development. *Proc. Natl. Acad. Sci.* **99**, 2240–2245.

Zipfel, P. A., Bunnell, S. C., Witherow, D. S., Gu, J. J., Chislock, E. M., Ring, C. and Pendergast, A. M. (2006). Role for the Abi/Wave protein complex in T cell receptor-mediated proliferation and cytoskeletal remodeling. *Curr. Biol.* **16**, 35–46.

Figures

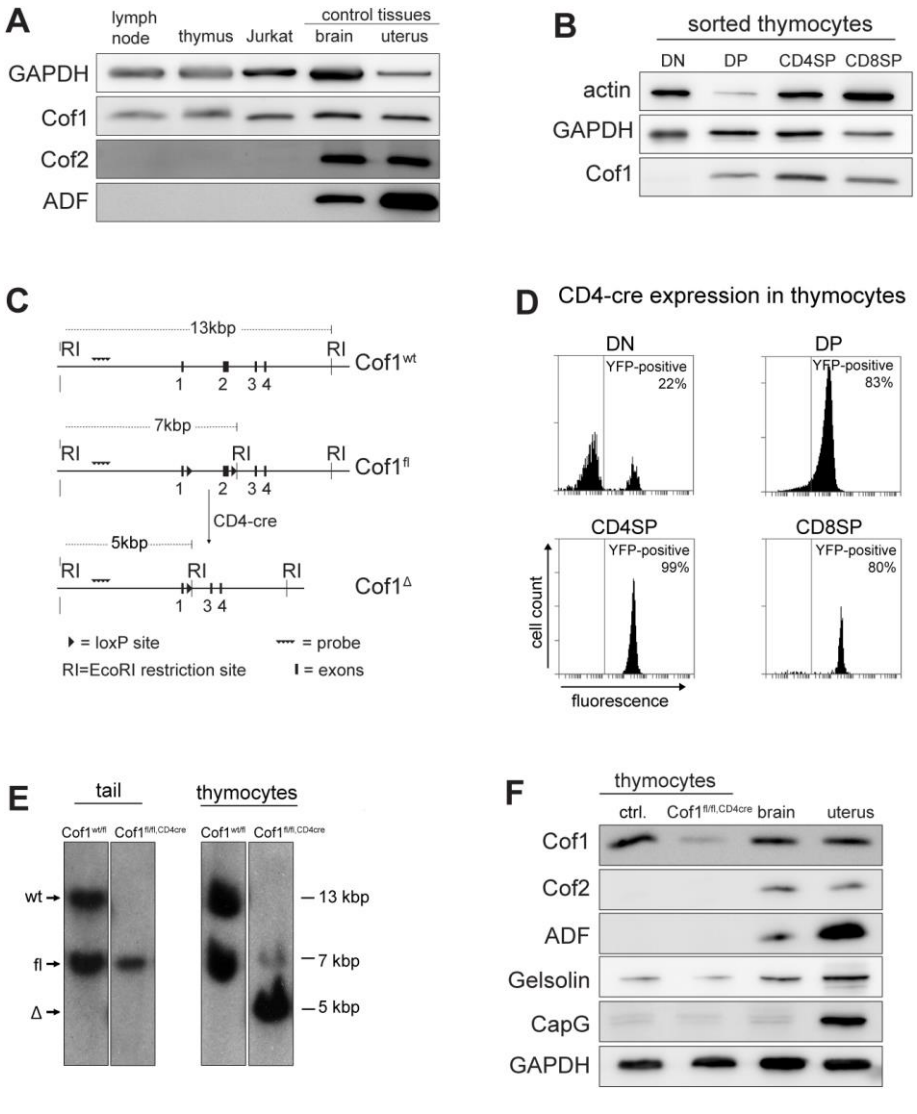

Figure 1: Thymocyte specific deletion of cofilin1.

(**A**) Western blot for ADF/cofilin family members in thymus and control tissues/cells. Cofilin1, cofilin2 and ADF were detected by isoform specific antibodies in total protein lysates from mouse lymph node, thymus, and Jurkat T cells. Brain and uterus are shown as positive controls for the antibodies. Note that lymphatic tissues and the Jurkat T cell line express only cofilin1 protein, but no cofilin2 and ADF. (**B**) Western blot of CD4- and CD8-sorted mouse thymocytes. Single cell suspension from thymus was sorted for CD4/CD8 double negative (DN), CD4/CD8 double positive (DP), CD4 single positive (CD4SP) and CD8 single positive (CD8SP) thymocytes. Lysates from equal cell numbers were loaded and probed for cofilin1 and actin, and GAPDH as

control. Note that DN cells express very low levels of cofilin1, and that DP cells contain the smallest amount of actin. (**C**) Cartoon of the wildtype ($Cof1^{wt}$), floxed conditional ($Cof1^{fl}$) and deleted ($Cof1^{\Delta}$) cofilin1 alleles. CD4-cre mediated recombination will delete exon2 in thymocytes and generate the knock-out allele ($Cof1^{\Delta}$); exons, loxP sites, diagnostic EcoRI sites and Southern blot probe are indicated. (**D**) Developmental control of CD4-cre mediated deletion in thymocyte subpopulations using a Rosa26-Stop-YFP^{CD4cre} reporter line. The vertical line in the histogram plots separates negative cells (left) and recombined, percent of YFP-positive cells (right). CD4-cre activity is already detectable at the DN stage, recombination increases at the DP stage, in CD4SP, and CD8SP cells. (**E**) Southern blot of control ($Cof1^{wt/fl}$) and $Cof1^{fl/fl,CD4cre}$ mouse DNA after EcoRI digestion shows efficient recombination and gene deletion (Δ) in $Cof1^{fl/fl,CD4cre}$ thymocytes, but no recombination in tail DNA used as controls. (**F**) Western blot analyses of cofilin1 protein depletion in total $Cof1^{fl/fl,CD4cre}$ thymocytes. Equal amounts of lysates from control (ctrl.) and mutant ($Cof1^{fl/fl,CD4cre}$) thymocytes, brain and uterus were loaded and probed with antibodies against cofilin1, cofilin2, ADF, gelsolin, CapG and GAPDH. Cofilin1 protein is strongly reduced in $Cof1^{fl/fl,CD4cre}$ thymocytes. Brain and uterus serve as positive controls for the antibodies. Experiments were repeated at least 3 times.

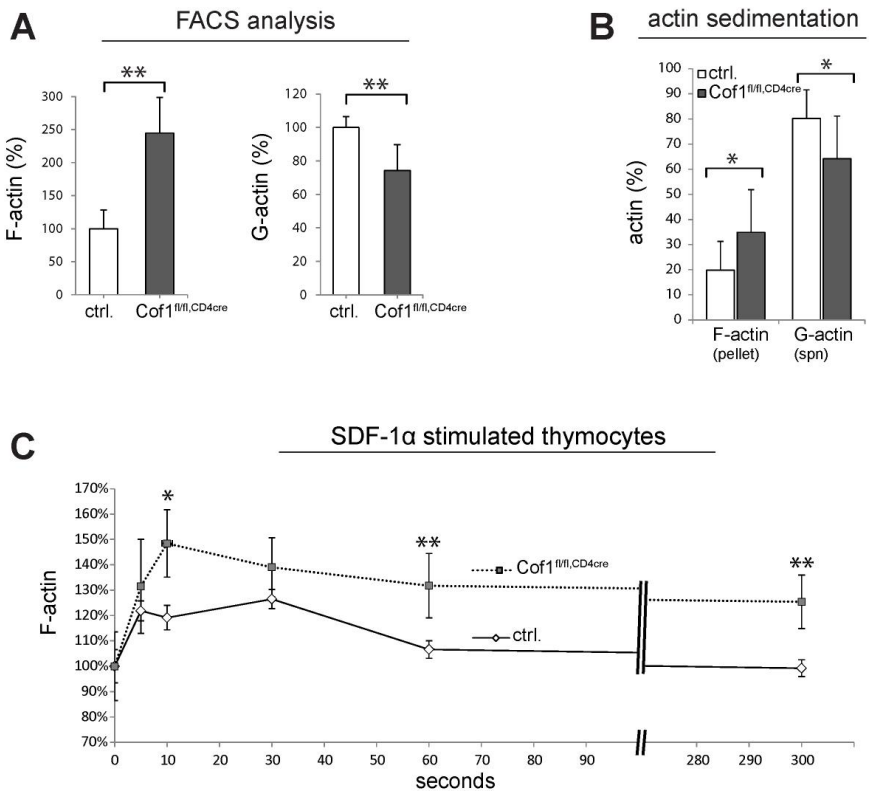

Figure 2: Actin filament dynamics in cofilin1 depleted thymocytes.

(**A**) Quantification of relative F- and G-actin levels in Cof1$^{fl/fl,CD4cre}$ thymocytes with respect to control thymocytes (ctrl.) using phalloidin/DNaseI staining and FACS analysis (n=7, standard deviations are shown with **0.001<P<0.01, unpaired two-tailed Students t-Test). In cofilin1 depleted thymocytes, F-actin was significantly increased and G-actin decreased. (**B**) Absolute amounts of Triton insoluble F- and Triton soluble G-actin were determined by high speed sedimentation and subsequent western blot analyses of control (n=4) and Cof1$^{fl/fl,CD4cre}$ (n=3) thymocytes. Cofilin1 depleted thymocytes showed increased F-actin (pellet) and decreased G-actin (spn) levels (standard deviations with *0.01<P<0.05; unpaired two-tailed Students t-Test). (**C**) F-actin dynamics in SDF-1α stimulated total thymocytes. F-actin was monitored by phalloidin staining and FACS analysis at the indicated time points after stimulation. The control is shown as solid line, cofilin1 depleted cells as dashed line. Values were normalized to unstimulated cells. Note that the data represent biological and not technical replicas (n=3 Cof1$^{fl/fl,CD4cre}$ and n=4 control mice, standard deviations are shown with *0.01<P<0.05; **0.001<P<0.01, unpaired two-tailed Students t-Test).

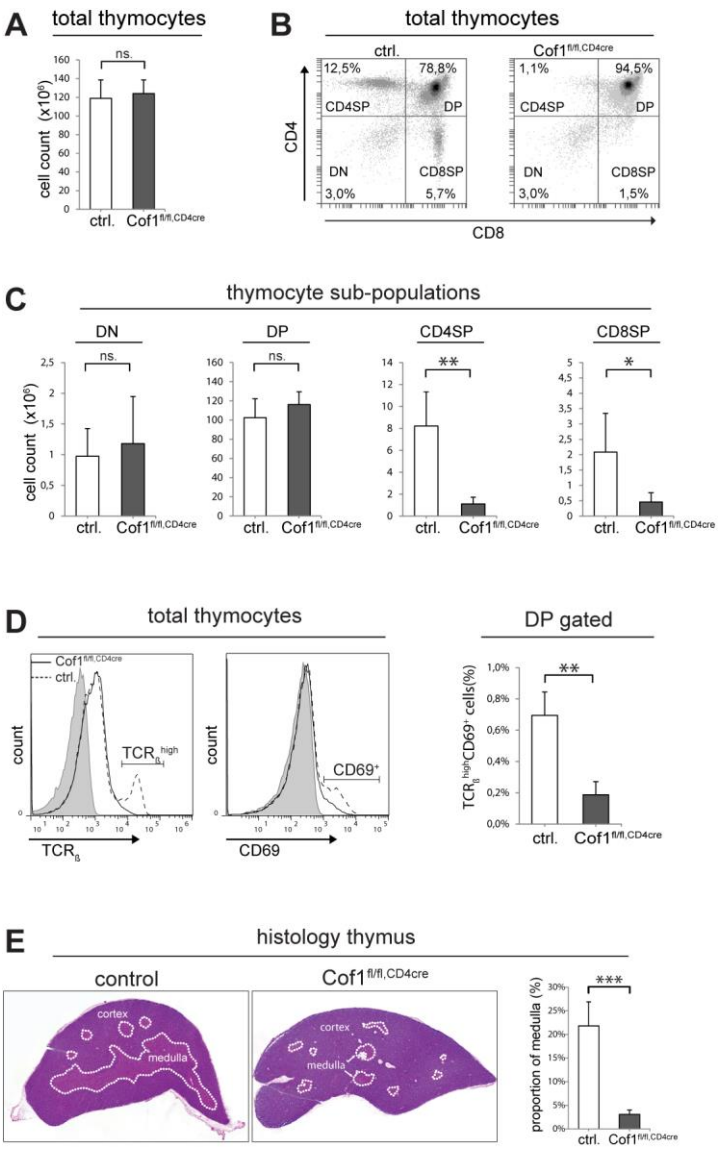

Figure 3: Single positive thymocytes were lacking in Cof1$^{fl/fl,CD4cre}$ mutant mice.

(**A**) The total number of thymocytes was comparable in control (ctrl.) and Cof1$^{fl/fl,CD4cre}$ mice (n=5). (**B**) FACS analysis of total control (ctrl.) and Cof1$^{fl/fl,CD4cre}$ thymocytes for CD4 and CD8, showing the differentiation block from DP cells to SP cells. CD4 and CD8 single positive thymocytes were decreased in Cof1$^{fl/fl,CD4cre}$ mice. Percentages of each cell population are given in the respective quadrants of the FACS plots. (**C**) Statistical analysis of thymocyte subpopulations. On average the number of DN and DP thymocytes were not altered in Cof1$^{fl/fl,CD4cre}$ mice, while CD4SP and CD8SP cells were severely reduced when compared to control mice (n=5). (**D**) Expression of TCRß receptor and CD69 in total thymocytes from control (dashed line) and Cof1$^{fl/fl,CD4cre}$ mice (solid lines). Histogram of FACS analysis is shown for TCRß^{high} and CD69^{+} thymocytes (left panel). Shaded curves represent unstained cells. Note that the

TCRß^{high}/CD69^{+} population is severely diminished in Cof1$^{fl/fl,CD4cre}$ mice. The bar chart (right panel) shows statistical analysis of TCRß^{high}CD69^{+} cells in the DP gated subpopulation (n=7). (**E**) The thymic medulla (white dotted lines) was reduced in adult Cof1$^{fl/fl,CD4cre}$ mice as shown by H&E staining of sections (left panel). Quantitation of the medullary area (right panel), relative to total thymus size (n=8). Statistical analysis: All histograms show standard deviations with ^{ns}0.05<P; *0.01<P<0.05; **0.001<P<0.01; ***P<0.001; unpaired two-tailed Students t-Test.

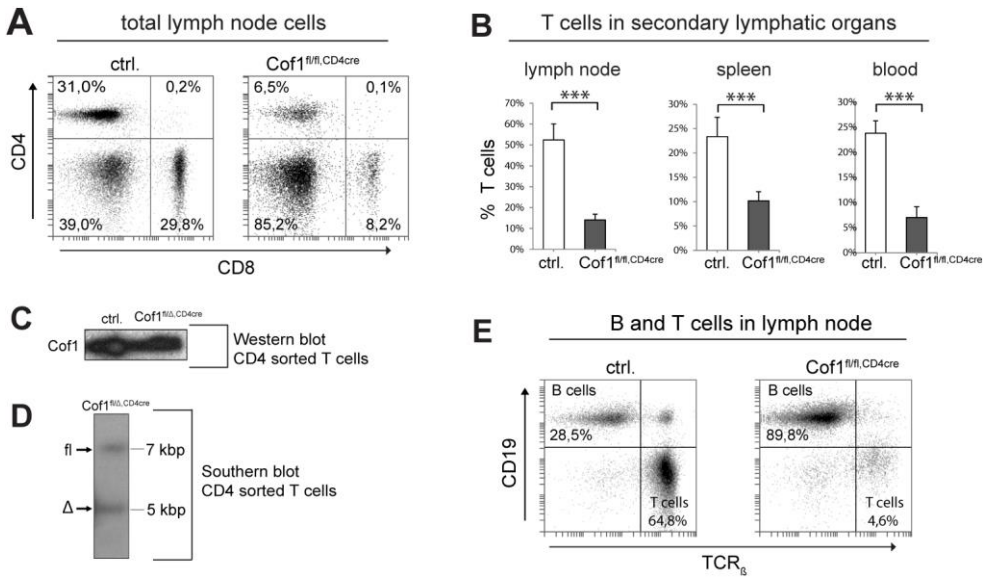

Figure 4: Thymocytes which escaped cofilin1 deletion differentiate into mature peripheral T cells.

(**A**) FACS analysis of lymph node cells showed the presence of CD4 and CD8 single positive T cells in the periphery of Cof1$^{fl/fl,CD4cre}$ mice. (**B**) Quantitation of peripheral T cells (lymph node, spleen, blood) with respect to total lymphocytes in control (ctrl.) and Cof1$^{fl/fl,CD4cre}$ mice (n=5, standard deviations are shown with ***P<0.001; unpaired two-tailed Students t-Test). (**C**) Western blot of CD4 sorted T cells from spleen confirmed normal expression levels of cofilin1 protein in peripheral T cells. Equal numbers of CD4 sorted cells from control (ctrl.) and Cof1$^{fl/\Delta,CD4cre}$ mice were loaded and the blot was probed with a cofilin1 specific antibody. (**D**) Southern blot analysis of genomic DNA from CD4 sorted T cells from Cof1$^{fl/\Delta,CD4cre}$ mice. Note that Cof1$^{fl/\Delta,CD4cre}$ mice are shown to directly illustrate the ratio of escaper cells in the periphery. The equal intensity of the fl and Δ alleles indicate that basically none of the fl-alleles was converted to the Δ allele and that the T cells found in the periphery had escaped cofilin1 gene deletion. (**E**) FACS analysis of B and T cell ratio in lymph nodes using CD19 as marker for B cells, and TCRß as marker for T cells (n=5).

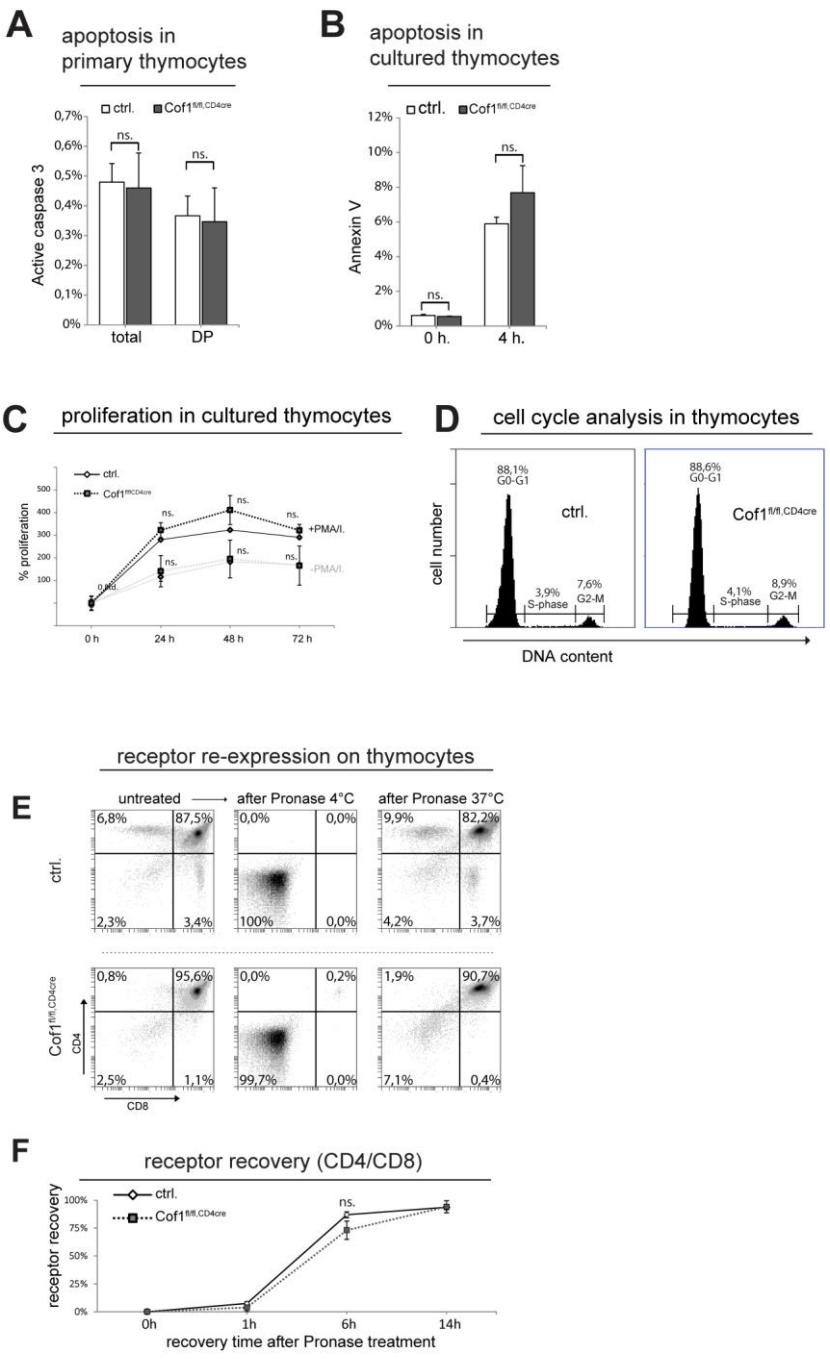

Figure 5: Apoptosis, cell proliferation and receptor transport in thymocytes is cofilin1 independent.

(**A**) Intracellular staining for active caspase 3 in total thymocytes and DP thymocytes. FACS analysis of control (ctrl.) and Cof1$^{fl/fl,CD4cre}$ thymocytes showed comparable percentages of apoptotic cells (n=3; standard deviation is shown; $^{ns}p<0,5$; unpaired two-tailed Students t-Test). (**B**) DP thymocytes kept in culture for 0h and 4h were analysed by FACS for the percentages of Annexin V positive cells (n=5; standard error is shown; $^{ns}p<0,5$; unpaired two-tailed Students t-Test). Note that prolonged culture

conditions increase the number of apoptotic cells equally in controls and Cof1$^{fl/fl,CD4cre}$ thymocytes. (**C**) Proliferation of total thymocytes after PMA/Ionomycin stimulation (+PMA/I) and without stimulation (-PMA/I). Under both conditions control thymocytes (black lines) and Cof1$^{fl/fl,CD4cre}$ thymocytes (grey lines) showed comparable expansion (n=8; standard error is shown; $^{ns}p<0,5$; unpaired two-tailed Students t-Test). (**D**) Cell cycle analysis of total thymocytes. DNA content was quantified by FACS analysis after staining cells with propidium iodide. The percentages of cells at different cell cycle stages was similar in control (ctrl.) and Cof1$^{fl/fl,CD4cre}$ thymocytes. (**E**) CD4 and CD8 surface expression on thymocytes was determined by FACS analysis before (untreated) and 14h after Pronase treatment either at 4°C or 37°C, respectively. Recovery of CD4/CD8 expression is shown in the upper right quadrant, and comparable at 37°C in control and Cof1$^{fl/fl,CD4cre}$ thymocytes. (**F**) Kinetics of CD4/CD8 receptor recovery from 0 to 14h after Pronase treatment in control (ctrl., black line) and Cof1$^{fl/fl,CD4cre}$ thymocytes (grey line) (n=5, diagram displays standard deviations; ^{ns} 0,05<P; unpaired two-tailed Students t-Test).

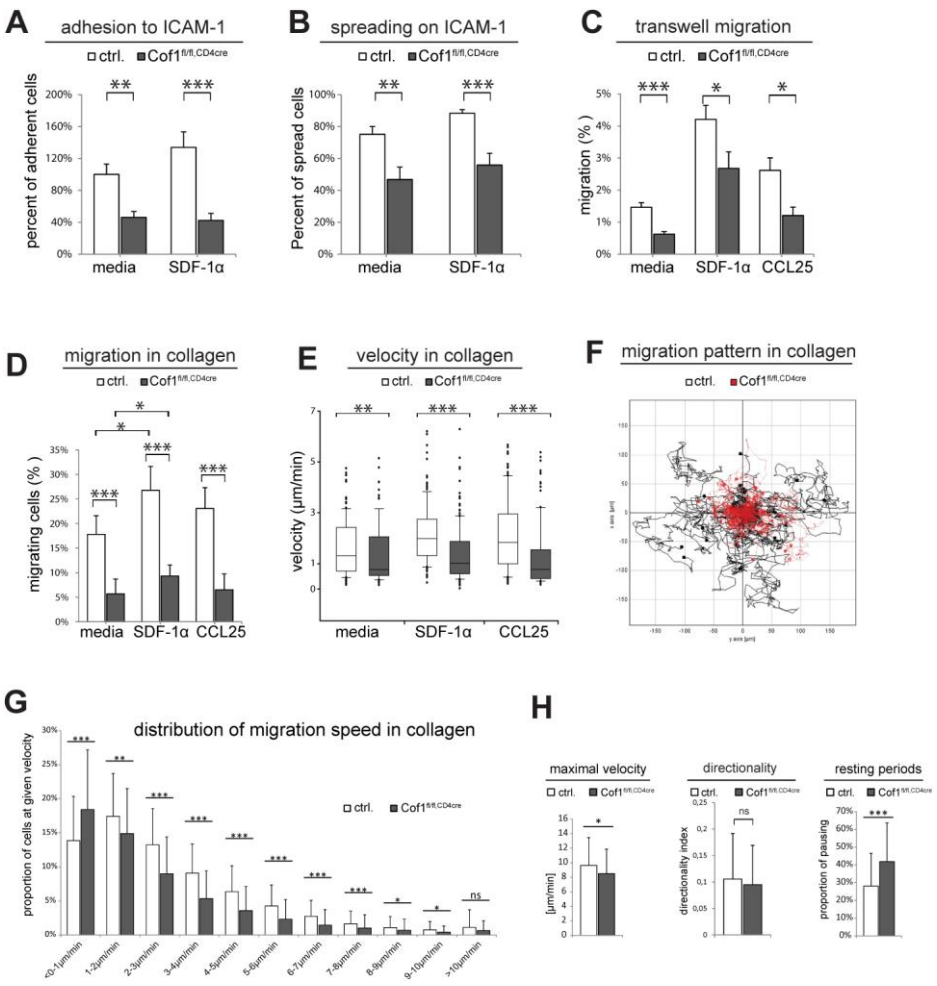

Figure 6: **Adhesion and migration were impaired in Cof1$^{fl/fl,CD4cre}$ thymocytes.**

(**A**) Adhesion and (**B**) spreading of control (ctrl.) and Cof1$^{fl/fl,CD4cre}$ thymocytes to ICAM-1 coated plates under resting conditions (media) or after SDF-1α stimulation. Adhesion and spreading were impaired in cofilin1 depleted thymocytes. (n=4; diagrams display standard error with **0.001<P<0.01;***P<0.001; unpaired two-tailed Students t-Test). (**C**) Transwell migration of thymocytes from control (ctrl.) and Cof1$^{fl/fl,CD4cre}$ mice in the absence (media) or presence of SDF-1α or CCL25 in the lower compartment. Percentages of cells that migrated to the lower chamber are shown (n=6). (**D**) Migration of control (ctrl.) and Cof1$^{fl/fl,CD4cre}$ thymocytes in a collagen gel either unstimulated (media) or stimulated by SDF-1α or CCL25. Migrating cells were analysed by time-lapse microscopy over 6h. (n=4). (**E**) Migration speed of control (ctrl.) and Cof1$^{fl/fl,CD4cre}$ thymocytes in collagen gel either unstimulated (media) or stimulated by SDF-1α or CCL25. Data are presented as whisker plots. Whiskers comprise 95% of data, dots indicate outliers. On average more than 120 cells were analysed per genotype and stimulation condition from 4 independent experiments. Significance was

calculated with the non-parametric Mann-Whitney Rank Sum test, normality of data was tested by Shapiro-Wilk test. (**F**) Random migration path of SDF1α stimulated control (black) and $Cof1^{fl/fl,CD4cre}$ (red) thymocytes in collagen. (**G**) Binning analysis of migration speed during a 6 hour period. Percent of time is shown which individual cells spent traveling at a given velocity within this period. (**H**) Maximal migration speed of control (ctrl.) and $Cof1^{fl/fl,CD4cre}$ thymocytes was comparable (left panel). The directionality index of SDF-1α stimulated migration in collagen gel was similar for control (ctrl.) and $Cof1^{fl/fl,CD4cre}$ thymocytes (middle panel). Proportion of resting periods in $Cof1^{fl/fl,CD4cre}$ thymocytes is significantly increased (right panel) (Statistics: n=144 ctrl. cells, n=182 $Cof1^{fl/fl,CD4cre}$ cells from 4 animals per genotype. All diagrams display standard deviations with $^{ns}0.05<P$; *0.01<P<0.05;**0.001<P<0.01;***P<0.001; unpaired two-tailed Students t-Test).

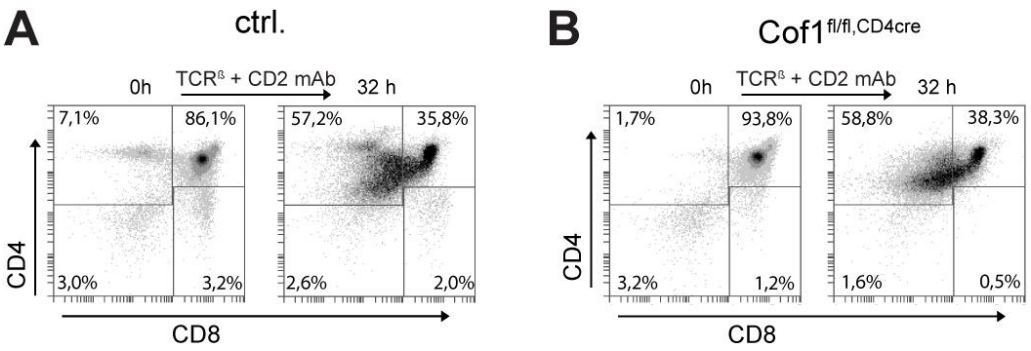

Figure 7: Cofilin1 deficient thymocytes differentiate *in vitro*.

(A, B) Control (ctrl.) and Cof1$^{fl/fl,CD4cre}$ thymocytes were cultured on TCRß and CD2 coated dishes and subsequently analysed by FACS. After 32h of culture both genotypes showed efficient differentiation of CD4/CD8 double positive thymocytes towards CD4 single positive cells (upper left quadrant). Percentages of cells in each quadrant are shown (n=6).

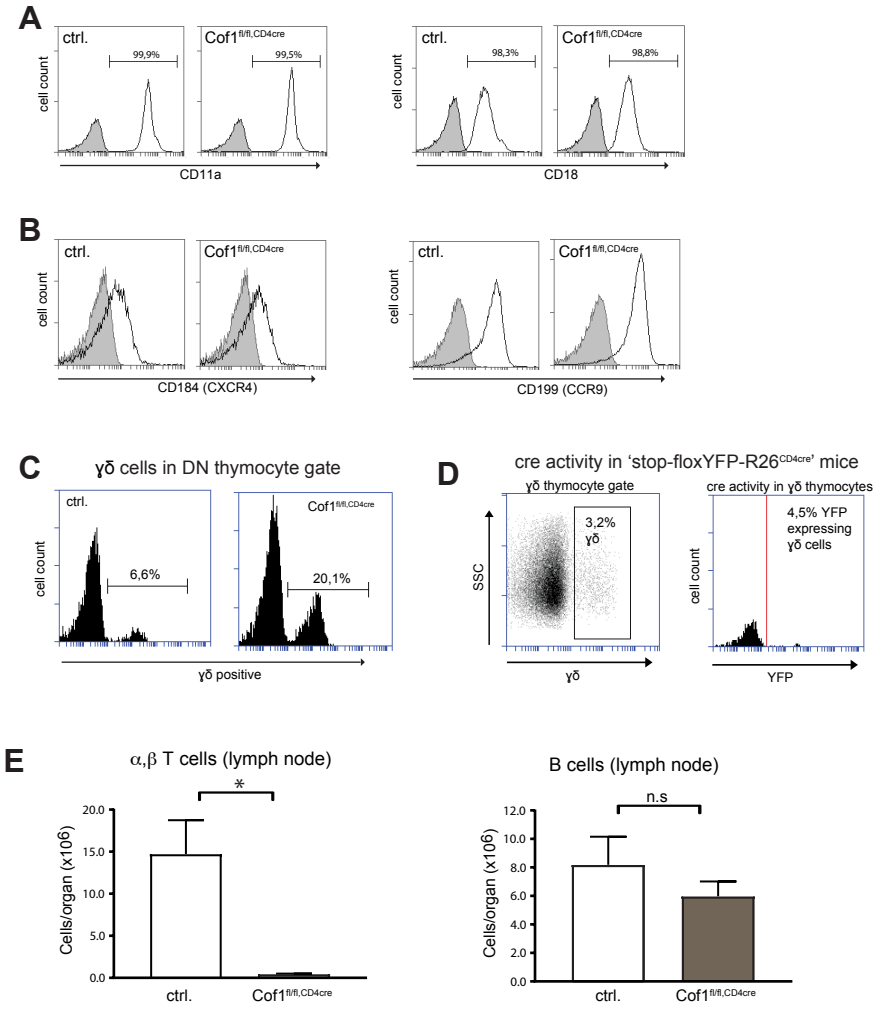

Figure S1

(**A**) Expression of extracellular ICAM-1 receptor chains CD11a and CD18 was comparable in DP thymocytes from control (ctrl.) and Cof1$^{fl/fl,CD4cre}$ mice. (**B**) Expression levels of chemokine receptors CD184 (CXCR4) for SDF-1α, and CD199 (CCR9) for CCL25 were comparable in DP thymocytes from control (ctrl.) and Cof1$^{fl/fl,CD4cre}$ mice. Analyses were performed by FACS. Grey peaks represent unstained cells (n=5). (**C**) Thymocytes were stained for γ,δ-chains and shown as percent of α,β DN cells. In Cof1$^{fl/fl,CD4cre}$ mice 20,1% of DN cells were γ,δ positive, while in controls (ctrl.) only 6,6% γ,δ positive cells were found. (**D**) In a Rosa26-Stop-YFP^{CD4cre} reporter mice, only 4,5% of of γ,δ cells were YFP positive, indicating that the CD4-cre transgene is only marginally expressed in γ,δ cells. Consequently the increased γ,δ cell number observed in **(C)** is due to a non-cell autonomous epiphenomenon. (**E**) The absolute numbers of CD19 positive B cells and CD4 positive T cells per organ were determined in lymph nodes of control (ctrl.) and Cof1$^{fl/fl,CD4cre}$ mice. Note that the absolute number of T cells, was reduced, while the absolute number of B cells was comparable in controls and mutants (Statistics: n=3, all diagrams display standard errors with $^{ns}0.05<P$; $*0.01<P<0.05$; unpaired two-tailed Students t-Test).